

Second Meeting of V3_4 DPC-INGV Project

Magma chambers. Geophysical, petrological and volcanological definition. Investigation methodologies and their intrinsic resolution. The Vesuvius problem.

INGV-Rome
13-14 October 2005

Introduction

On October 13-14 the second meeting of V3_4 DPC INGV Project was held in Rome-INGV from 11.30 of thursday 13th up to 17.00 of friday 14th.

The theme of the meeting was ""Magma chambers. Geophysical, petrological and volcanological definition. Investigation methodologies and their intrinsic resolution. The Vesuvius problem". This argument was solicited during the first kick-off meeting held in Naples on July 7-8, where several main items appeared of some importance to all the participants:

- a) Is there any definition of magma chamber that is transversal to all the disciplines in Volcanology?
- b) Where are, if any, the actual magma chambers of Mt. Vesuvius?
- c) Are the results obtained inside the different disciplines, comparable or in contrast?
- d) How the magma chambers may be dynamically related to the next eruptive activity of Mt. Vesuvius?

To answer to all these questions the organizers decided to give to the meeting the cut and thrust of a "brainstorming" debate, based on few talks given by the operators of the project who were the most involved in the arguments solicited.

The result was beyond all the expectations. A great effort was done first to unify the definitions and give the uncertainties; then to look for a unifying vision among the different point of views, and finally to plan multidisciplinary approaches.

Gravimetric methods and their resolution

Giovanna BERRINO*

*INGV- Osservatorio Vesuviano, Via Diocleziano 328. Napoli. Tel: +39 081 6108307; fax: +39 081 6108351; e-mail: berrino@ov.ingv.it

1. Introduction

The aim of Gravity is to determine the gravity field of the Earth.

Gravity, which has to be measured on the surface of the Earth, contains information about mass distribution in the interior of the Earth; that is, about density distribution. Therefore, gravity in geophysics permits to determine the structural setting of the investigated area.

Theoretically, gravity can define disturbing masses of any dimensions, at any depth and with any density contrast. Disturbing masses (i.e., density differences - positive or negative - $\Delta\rho$) can be determined through "gravity anomalies" which can be derived by gravity measurements. Gravity anomalies can be defined as a disturbing quantity of the gravity field. Therefore, they are defined as the difference between the measured gravity value and the "normal gravity value" deriving from the theory at the same point: $\Delta g = g_{\text{obs}} - g_{\text{theo}}$

This comparison is complicated by the fact that the observation contains the integral effect of all masses and that g_{obs} and g_{theo} are referred at two different surfaces. Therefore, the influence of height and of interposed masses would be removing by reductions.

Uncertainties in the reduction are introduced mainly by:

- Deviation of free-air reduction (height reduction) computed with a normal value from the true value;
- Inadequate topography model for terrain correction
- Uncertainty on density value for mass reduction

The reduced anomaly is normally known as "Bouguer gravity anomaly" and it is generally used for the development of regional and local density models. The Bouguer anomalies are expressed in an auxiliary unit: milliGal ($1\text{mGal} = 10^{-5} \text{ms}^{-2}$). Global uncertainty on the Bouguer gravity anomaly generally ranges from 0.1 to 1 mGal ($10^{-6} \dots 10^{-5} \text{ms}^{-2}$).

This restricts the gravity potential, so that at best gravimetry is able to determine density differences with an uncertainty of $\pm 50 \dots 200 \text{kg/m}^3$ and depths of disturbing masses with an uncertainty of $\pm 5 \dots 20\%$. Limits are also introduced by the space structure of the field survey (i.e., extension of networks) and by density of gravity measurements (i.e., number of stations and distances among stations).

The more the disturbing mass is deep, the more the surface effect is extended. Generally, the ratio between depth and dimension of the source and extension of anomaly is about 1:10; e.g.:

- A source some meters long, at a depth of some meters will generate an anomaly extended dozens of meters;
- A source some kilometres long, at a depth of some kilometres will generate an anomaly extended dozens of kilometres;
- Crustal sources will generate anomalies extended hundreds of kilometres.

In order for gravimetry to make sense, the dimension of the disturbing masses in depth, extension and density contrast relative to the adjacent rocks must be large enough to produce observable gravity anomalies.

In the case of Magma Chambers, gravity is not really able to detect any simple magma system because, being it almost neutrally buoyant, has very small density contrast with the host rocks. Therefore, resulting gravity anomalies are subtle to detect among background anomalies.

2. Simulation

Simulations have been made through the "direct problem of gravimetry" (i.e., the computation of the gravitation generated by a particular mass distribution given in terms of location, shape and density, in this case, density contrast $\Delta\rho$) to compute the gravity anomaly generated by a magma chamber.

In the general case, a magma chamber has been assumed as a spherical and homogenous body, having a density contrast with the surrounding medium of $+100 \text{kg/m}^3$. It is obviously that the same source with a negative density contrast will generate the same anomaly with opposite sign. The simulation has been made with two sources having a radius of 500 and 1000 m, respectively, at several depths. Results are shown in the Figure 1, where it is evident that only the source with a radius of 1000 m and its top at 500 m gives a significant gravity signal. The rest give a very small gravity signal or at worst close to the data uncertainty.

Simulation of a spherical source $\Delta\rho = +100 \text{ kg/m}^3$

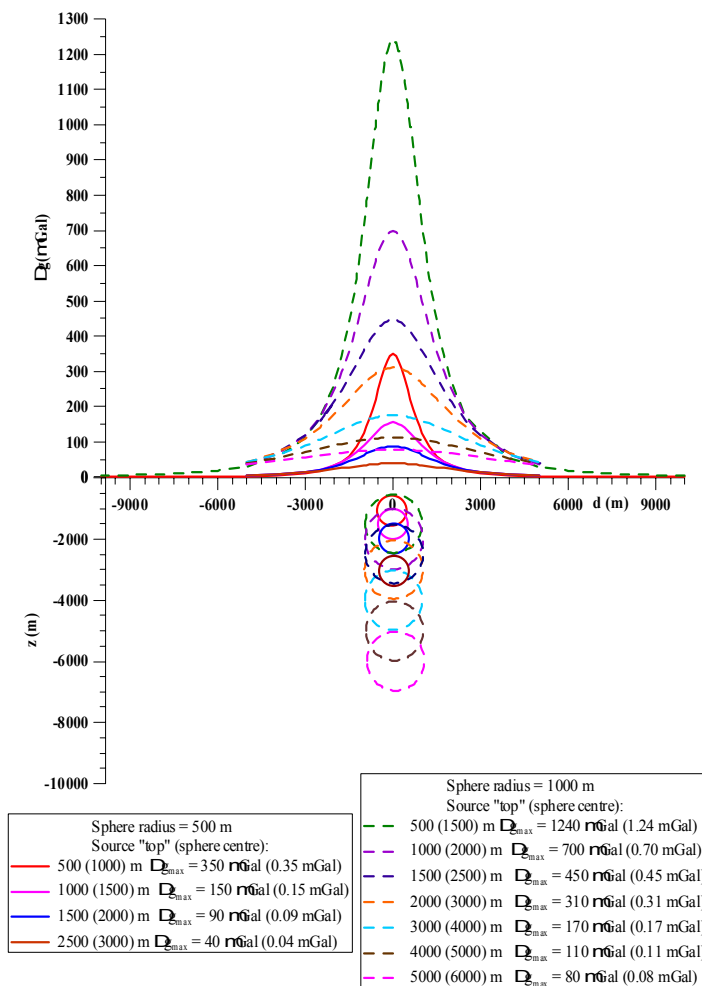


Figure 1

In the case of Vesuvius, the simulation has been made taking separately into account the shape and the depth of a shallow and a deep magma chambers as suggested by petrological and seismic studies. All simulations have been made along two profiles, respectively W-E and S-N, both crossing the top of Mt. Vesuvius, also accounting for the topographic profile of Mt. Vesuvius.

To simulate the largest gravimetric effect of a shallow magma chamber, the model of the magma chamber before the A.D. 79 Plinian eruption (from Santacroce et al., 1996) has been taken into account; it has been positioned below the crater and considered as a homogeneous sphere, with:

Volume = $2 \cdot 10^9 \text{ m}^3$; Radius = 800m and 1000m; Top = $\sim 4 \text{ km}$; Density $\rho = 2200 - 2500 \text{ kg/m}^3$

Taking into account a density of about 2500 kg/m^3 of host rocks, a realistic density contrast $\Delta\rho$ of -100 kg/m^3 has been used in the computation.

Results are shown in the Figure 2 (left). Such a kind of magma chamber generates a very small gravity anomaly (maximum value about $-40 \text{ } \mu\text{Gal} = -0.04 \text{ mGal}$). Even if the radius of the chamber is increased to 1000 m, no significant gravity anomaly is obtained (maximum value is of about $-80 \text{ } \mu\text{Gal} = -0.08 \text{ mGal}$). The simulation has been also made increasing density contrast up to not realistic values of -400 kg/m^3 ; also in this case the obtained gravity anomaly is inside the uncertainty.

To simulate the deep magma chamber, results of new seismic tomography (Auger et al., 2001) have been taken into account; also accounting it has been used to compute the thermal state of Vesuvius (Civetta et al., 2004). So that a "Sill shaped" chamber has simulated, with:

Length = 20 km; Width = 20 km; Thickness = 2 km; Top of the source = 8 km; $\Delta\rho = -100 \text{ kg/m}^3$

The computation has been made along the same profiles as above and results are shown in the Figure 2 (right). A significant anomaly, of about 3 mGal, is generated by this kind of source, but it doesn't appear in the real gravity anomaly field as measured on Mt. Vesuvius. Red and blue continuous lines in the upper figure represent the theoretical anomaly generated by the source at the sea level.

Spherical sources with:
radius = 800 m; **radius = 1000 m**
Depth of the sphere centre = 5000 m [top = 4200; 4000 m]
density contrast = - 100 kg/m³

Sill source with:
Lenght (along x axis W-E) = 20000 m [a = 10000 m]
Width (along y axis S-N) = 20000 m [b = 10000 m]
Thickness (along z axis - depth) = 2000 m [c = 1000 m]
Depth of the source centre = 9000 m [top = 8000 m]

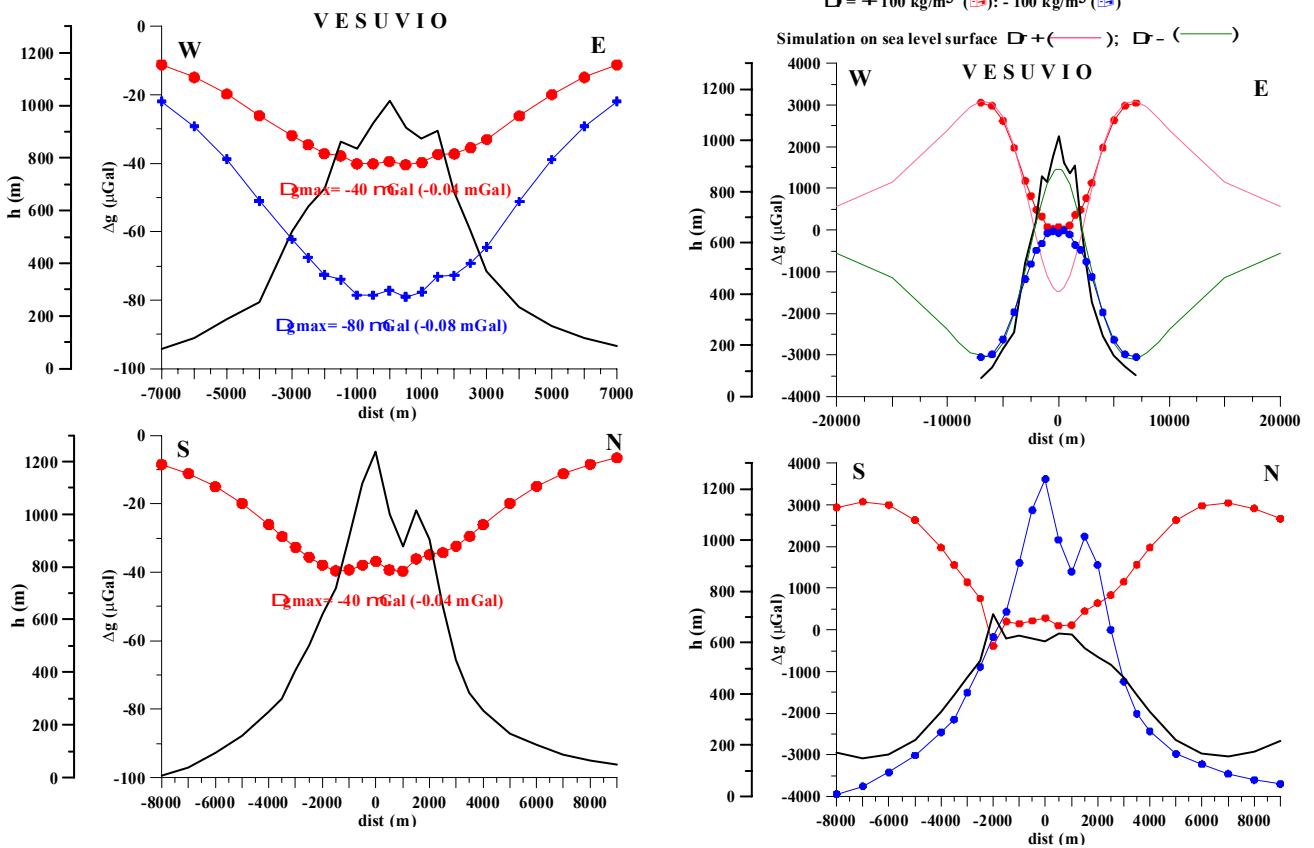


Figure 2

3. Conclusions

Gravity anomalies required to be computed with uncertainties of few microGal to detect magma chambers with linear dimension of some kilometres, at a depth up to 10 km and with small density contrast (of the order of 100 kg/m³). Therefore, it is necessary: a dense gravity network extended dozens of kilometres, height of gravity stations measured with sub-cm accuracy, distance among stations of the order of hundred of meters; availability of a detailed digital topography map to improve the terrain correction; well known geological setting of the investigated area; well known “regional” gravity model.

Direct measurements of the vertical gravity gradient on a dense network could provide more meaningful results. Vertical gravity gradient, even if considerably affected by topography, is more sensitive to later density variation (i.e., density variation between magma chamber and surrounding rocks) and remove (or reduce) the “regional” effect.

4. References

- Auger E., Gasparini P., Virieux J., Zollo A., 2001. Seismic evidence of an extended magmatic sill under Mt. Vesuvius. *Science*, 294, 1510-1512.
- Civetta L., D'Antonio M., de Lorenzo S., Di Renzo V., Gasparini P., 2004. Thermal and geochemical constrain on the “deep” magmatic structure of Mt. Vesuvius. *J. Volcanol. Geotherm. Res.*, 133, 1-12.
- Santacroce R., Cioni R., Marianelli P., Sbrana S., 1996. Discussing the Vesuvius model of operation on the base of petrochemical data. In “Vesuvius – Decade Volcano” Workshop Handbook, 14-33
- Encyclopedia of Volcanoes, 2000. Ed. H. Sigurdsson. Academic Press, pp. 1417.
- Torge W., 1989. Gravimetry. Walter de Gruyter, Berlin-New York, pp. 465

Stress Variations related to the magma ascent and their detection through seismological methods

Francesca Bianco

Istituto Nazionale di Geofisica Vulcanologia - Osservatorio Vesuviano

The Stress Field acting on a particular area may be obtained, from seismological studies, directly from the analysis of seismic data retrieving the following parameters:

- stress tensor through the inversion of the fault plane solutions
- splitting parameters through the quantitative analysis of the waveforms

These parameters are generally obtained through two different approaches, involving studies of seismic sources the first, and studies on the propagation in complex medium the second. Both approaches allow for static and dynamic measurements of the stress-field

- Stress tensor inversion

In order to calculate the stress tensor two main assumptions are needed : 1) the uniformity of the stress field in the analyzed area; Stress and Strain are coaxial in the area under consideration.

The input data are the fault plane solutions, that are processed by groups, in peculiar inversion schemes. The more used inversion scheme is the one proposed by Gephart (1990), hereafter referred to as FMSI. FMSI performs a grid search to find the best fit stress tensor for a given population of fault plane solutions by identifying the stress tensor with the lowest average misfit. As usual when inverting techniques are applied the results, that are Principal Stress Orientation and relative stress magnitude- s_1 , s_2 , s_3 , depend on the starting model; this dependence must be checked through successive inversions.

The knowledge of the stress variations before and after an eruption is a very interesting task. Roman et al. (2004) studied the temporal variation of the local stress field before and after the 1992 eruptions at Mount Spurr, Alaska, evidencing that the magmatic activity induced a measurable rotation of the stress field that the authors explained as resulted from the pressurization of a network of dykes.

This simple example suggests that this kind of studies allow to infer the dynamical state of a volcano system and to interpret this information in a volcanological way.

-Splitting Parameters

Shear wave splitting is the elastic analogue of the well known optical birefringence phenomenon. When a shear wave enters an anisotropic solid, it splits into two different quasi shear waves with different velocities and approximately orthogonal polarizations (Crampin 1981). The two diagnostic properties are ϕ , the azimuthal polarization of the faster split shear-wave in the horizontal plane, and δt , the time-delay between the split shear-waves. In the framework of the APE (Zatsepin & Crampin 1997), both the splitting parameters give informations on the stress field acting in the area; in particular, ϕ is an indirect measure of the direction of the maximum compressive stress field, whilst δt measures its intensity. Generally the cause of the stress-aligned shear-wave splitting observed throughout the crust is the distribution of fluid-saturated grain-boundary cracks and aligned pores in almost all rocks in the crust. Such fluid-saturated microcracks are highly compliant and are aligned by the stress field into typically parallel vertical orientations. The evolution of such fluid-saturated cracks under deformation can be calculated by the anisotropic poro-elasticity (APE) model of fluid-rock deformation, where the driving mechanism is fluid migration by flow or diffusion along pressure gradients between microcracks at different orientations to the stress-field. According to this scheme the splitting parameters monitor the variation of the stress field, and may be referred to as a new class of precursors for impending earthquakes and/or eruptions.

Due to their features the fluid-saturated microcracks are highly sensitive also to small changes in the stress. As example, both δt and ϕ have been observed to change at least 20 days before the M=3.6 earthquake (9 October 1999)

In our opinion, the shear wave splitting parameters may be continuously monitored in order to detect in advance all the variations of the stress field acting on a volcano possibly prelude to magma uprising.

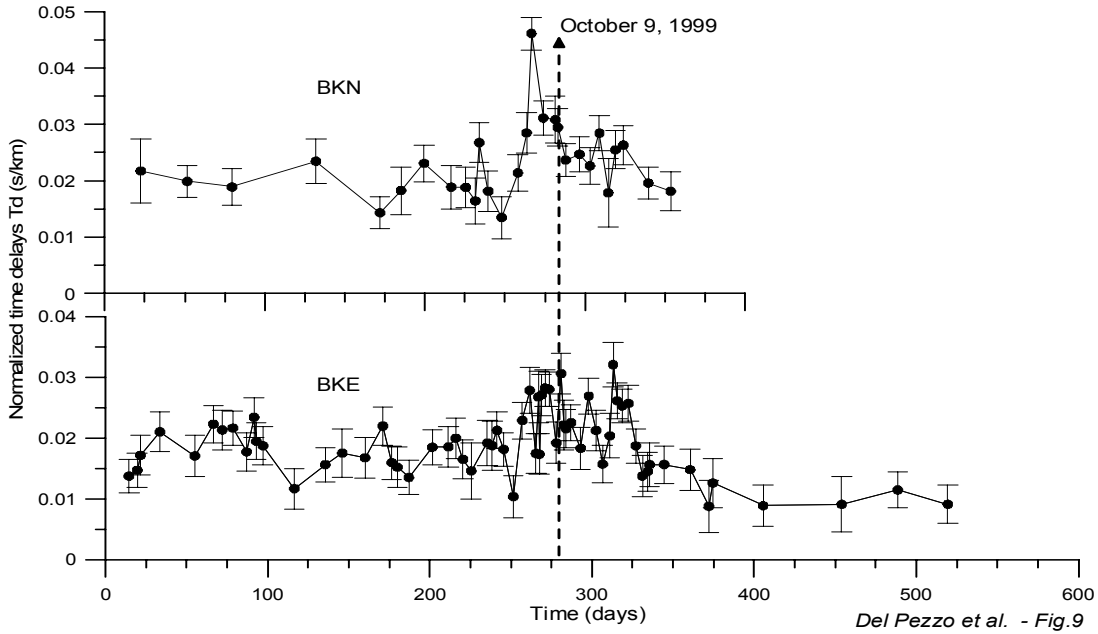
References

- Crampin, S., 1981. A review of wave motion in anisotropic and cracked elastic-media, *Wave Motion*, 3, 343-391.
- Del Pezzo, E., Bianco, F., Petrosino, S. & Saccorotti, G., 2004. Changes in the coda decay rate and shear wave splitting parameters associated to seismic swarms at Mt. Vesuvius, Italy, *Bull. Seism. Soc. Am.*, 94, 439-452.
- Gephart, J.W., (1990). FMSI: a fortran program for inverting fault/slickenside and earthquake focal

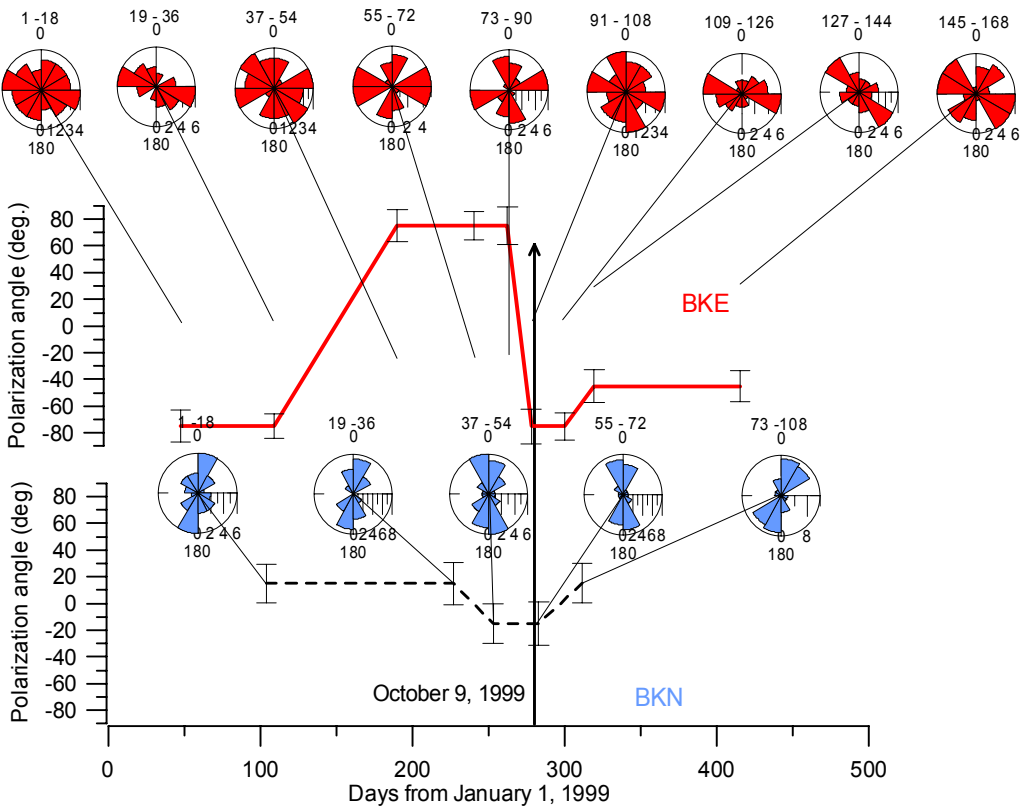
mechanism data to obtain the regional stress tensor. *Computer & Geosciences*, 16,7, 953 - 989.

Roman, D.C., Moran, S.C. Power, J. A. and K.V. Cashman, (2004). Temporal and spatial variation of local stress fields before and after the 1992 eruptions of Crater Peack Vent, Mount Spurr, Alaska. *Bull Seism. Soc. Am.*, 94,6 2366-2379.

Zatsepin S. V. & Crampin, S., 1997. Modelling the compliance of crustal rock: I - response of shear-wave splitting to differential stress, *Geophys. J. Int.* 129, 477-494.



Del Pezzo et al. - Fig.9



Del Pezzo et al. - Fig.10

Timing and styles of crystallization and degassing during syn-eruptive ascent of alkaline magmas

Raffaello Cioni

Dip.to Scienze della Terra, Via Trentino, Cagliari

rcioni@unica.it

The dynamics of magma ascent during explosive and effusive eruptions has been the subject of several studies in the last few years. The problem has been addressed in some different ways: physical and numerical modeling of conduit flow (Papale 2001, Mastin and Ghiorso 2000, Melnik 2000), analogue modeling of magma vesiculation and fragmentation during ascent (Mader et al 1994, Martel et al 2000), and textural studies of the products related to different eruptive styles and magma compositions (Cashman 1990, Cashman and Blundy 2000, Nakada and Motomura 1995).

The process of magma ascent is characterised by decompression, magma degassing and degassing-induced crystallization. The extent to which the process proceeds is strongly dependent on the rate of magma rise and on the rheological and compositional features of the magma. Important information about the process of magma ascent can be collected by studying the textural features of past eruptions and their variations with time within the eruption itself. In particular, by studying the shape, size and frequency distribution of vesicles and groundmass crystals inferences can be made on the modality and rates of magma ascent to the surface. This can be coupled with the results of experimental petrology experiments aimed at reproducing the observed mineral assemblages of the groundmass and distribution of volatile species. The results of these studies can be used to infer the conditions of final magma ascent to the surface in terms of times, magma rheology and evolution and composition of the exsolving volatiles. All these data can also be used to define more precisely, together with the results deriving from experimental petrology, the crystallization history within the magma chamber.

Very few data exists on the dynamics of syn-eruptive magma vesiculation and crystallization of alkaline magmas. Data on phonolitic and trachytic compositions have been recently collected studying some eruptions from Vesuvius and Phlegrean Fields. In particular, textural studies of pumice and scoria were done on the AD 79 Vesuvius and AD 1538 Phlegrean Fields eruptions (Gurioli et al., 2004; D'Oriano et al., 2004).

Some important problems which can be addressed with the above mentioned studies are the following:

- The definition of the likely conditions of pre- and syn-eruption magma degassing and crystallization.
- The possible timing of the onset of magma ascent during past eruptions, in order to define the expected precursors of an impending eruption

Timescales of magma crystallization in phonolitic and trachytic magmas

Data on the rates of magma crystallization during the eruption of alkaline magmas are very rare. The scientific literature has widely addressed this topic for what concerns calc-alkaline products. Basaltic compositions have been largely investigated as well, especially regarding the vesiculation processes. Recently, data have been collected on evolved compositions from both Vesuvius and Phlegrean Fields (Gurioli et al., 2004; D'Oriano et al., 2005). The most important indication deriving from these data is that groundmass crystallization occurred in very short times (hours to one or two days) before and/or during the studied eruptions. An important result preliminarily presented in Gurioli et al. (2004) is that also the very initial products of the AD 79 Vesuvius eruption are characterised by a population of groundmass crystals (Fig. 1) which records a growth history started at least a couple of days before the eruption. A similar indication is also recorded in the initial products of the AD 1538 Monte Nuovo eruption of Phlegrean Fields (D'Oriano et al., 2005). This suggests that the detailed study of these initial phases of some past eruptions can give important information on the style and timing of final magma ascent toward the surface.

The preliminary results on alkaline magmas suggest that degassing-induced crystallization can be very efficient and fast. The kinetics of magma crystallization and degassing represents an important difference in the dynamics of alkaline vs. calc-alkaline eruptions and may have strong influence on conduit processes. This results from the lower viscosity of alkaline magmas with respect to their calc-alkaline counterparts. Furthermore, as feldspar-feldspathoid composition for trachytic-phonolitic melts is very close to that of the residual liquid, feldspar-feldspathoid crystallization does not significantly affect the residual liquid, impeding the significant, compositionally driven melt viscosity increase which characterizes the final stages of crystallization of calc-alkaline magmas. The lower viscosity of the alkaline residual melts likely contributes to maintain high crystal growth rates and an efficient degassing also during the final stages of crystallization.

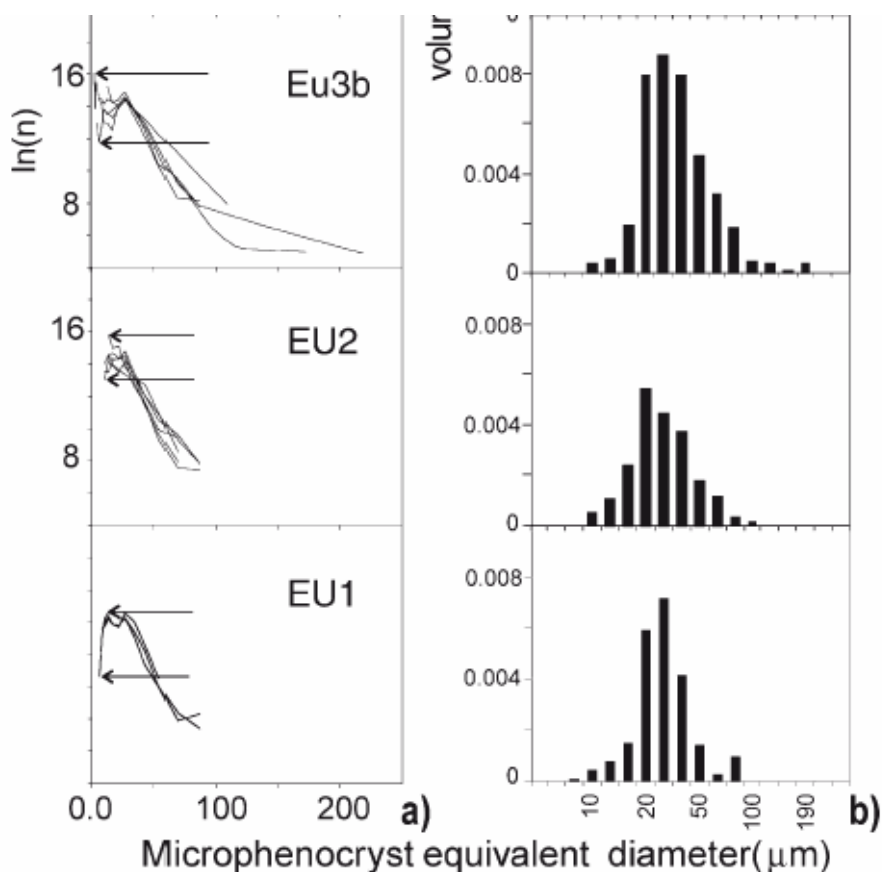


Fig. 1 Crystal size distribution of leucite microphenocrysts from the AD 79 Vesuvius eruption. A general increase in average crystal size can be noted from the base upward. Pumices from very initial phases of the eruption (EU1) show a smaller average size than white pumice (EU2), suggesting that leucite from the groundmass started nucleating and growing a few days before the eruption (after Gurioli et al. 2004)

References

- Cashman KV, Blundy J. 2000. Degassing and crystallization of ascending andesite and dacite. *Phil. Trans. R. Soc. Lond. A*, 358, 1487-1513
- Cashman, K. V. 1990 Textural constraints on the kinetics of crystallization of igneous rocks. *Rev. Mineral.* 24, 259-314.
- D'Oriano C, E. Poggianti, A. Bertagnini, R. Cioni, P. Landi, M. Polacci, M. Rosi 2005. Changes in eruptive style during the A.D. 1538 Monte Nuovo eruption (Phlegrean Fields, Italy): the role of syn-eruptive crystallization. *Bull Volcanol* 67:601–621, DOI 10.1007/s00445-004-0397-z
- Gurioli L. Houghton B., Cashman K., Cioni R. 2004. Complex changes in eruption dynamics and the transition between Plinian and phreatomagmatic activity during the 79 AD eruption of Vesuvius. *Bull. Volcanol* DOI: 10.1007/s00445-004-0368-4
- Mader H, Zhang Y., Phillips J.C., Sparks R.S.J., Sturtevant B., Stolper E., Experimental simulations of explosive degassing of magma, *Nature* 372 (1994) 85-88.
- Martel C, Dingwell D.B., Spieler O, M. Pichavant M, Wilke M (2000) Fragmentation of foamed silicic melts: an experimental study *Earth and Planetary Science Letters* 178 47-58
- Mastin L.G., Ghiroso M.S., 2000. A numerical program for steady-state flow of magma-gas mixtures through vertical eruptive conduits. *U.S. Geological Survey Open-File Rep. 00-209*, 53 pp.
- Mastrolorenzo, G., Brachi, L., Canzanella, A., 2001. Vesicularity of various types of pyroclastic deposits of Campi Flegrei volcanic field: evidence of analogies in magma rise and vesiculation mechanisms. *J. Volcanol. Geotherm. Res.* 109, 41– 53.
- Melnik, O. E. 2000, Dynamics of two-phase conduit flow of high-viscosity gas-saturated magma: Large variations of sustained explosive eruption intensity, *Bull. Volcanol.*, 62, 153–170.
- Nakada, S. & Motomura, Y. 1999 Petrology of the 1991{1995 eruption at Unzen: effusion pulsation and groundmass crystallization. *J. Volcanol. Geotherm. Res.* 89, 173-196.
- Papale, P., 2001. Dynamics of magma flow in volcanic conduits with variable fragmentation efficiency and nonequilibrium pumice degassing. *Journal of Geophysical Research, [Solid Earth]* 106, 11043– 11065.

SUB Project V3-4 Vesuvio

Task 1: the volcanic structure and magma feeding system.

RU: Civetta

The project is aimed at defining the deep and shallow volcanic structure, related to the main Plinian (Mercato and Avellino) and sub-Plinian (1631) Vesuvius eruptions, to identify the magmatic components present in the reservoirs and the new arrivals of deep magma, and their possible role in triggering eruptions. The results of the geochemical, isotopic and mineralogical studies on the Vesuvius products carried out in the last months, as well as the results of 2D conductive thermal model, have shown that:

- 1) Vesuvius magma source is in the asthenospheric mantle partially modified by fluids from the N - W subducted Ionian plate (Di Renzo et al., submitted);
- 2) the results of a Vesuvius 2D thermal model reproduce the present state of the thermal field of the deep magmatic reservoir 10km x 2km, situated at 8km of depth, after a periodical refilling since 400 ka, with a final magma input of 5 km², 40 ka ago (de Lorenzo et al., in preparation);
- 3) in the deep reservoir, which must extend discontinuously, mantle derived magmas stagnate, differentiate and are contaminated with the continental crust (Di Renzo et al., submitted);
- 4) from the deep reservoir (8 km or more) isotopically distinct magmas rose at shallower depth and formed, in the past, Plinian and sub-Plinian magma chambers, where they mixed with the resident magmas left by the previous eruption;
- 5) mixing/mingling is a very common process in the Vesuvius shallow magma chambers;
- 6) the result of geochemical, isotopic and mineralogical studies carried out on the products of Mercato eruptions 8 ka (Aulinas et al., in preparation) evidence that the erupted phonolitic magma is fairly homogeneous in chemical and isotopic composition, is in isotopic equilibrium with the separate mineralogical phases, with the exception of the Mg-rich cpx, which is progressively more enriched in radiogenic Sr during the course of eruption. Comparison between Mercato and Avellino (3.7 ka) chemical and isotopic compositions, shows that the two eruptions probably progressively tapped the same reservoir, the most phonolitic upper part being extruded during the Mercato eruption, and the last differentiated phonolite to phonotephrite portion during the Avellino eruption;
- 7) the products of Pollena eruption - 472 AD (Font et al.,in preparation), conversely, show a progressive change in chemical and isotopic composition during the course of eruption, clearly indicating the arrival of last-differentiated more-radiogenic magma before the eruption, which mix/mingles with the resident one;
- 8) the new isotopic data relative to Mercato and Pollena, and data from the literature, reported versus the age of eruption in the following figure, show that, isotopically distinct magmas rise from a deeper depth to form Plinian and sub-Plinian magma reservoirs. The same isotopic trend through time shown by the Mercato and Avellino products, is a good evidence of the existence of a same isotopically and compositionally stratified reservoir progressively tapped during the two eruptions.

Open Problems

One of the major open problems is the relation between the deep magma chamber, identified by seismic tomography and the Mercato, Avellino and Pompei Plinian magma chambers, in terms of depth.

One of the major open problem is the relation between the closed and open conduit conditions. What is the cause which determines the transition between the two conditions.

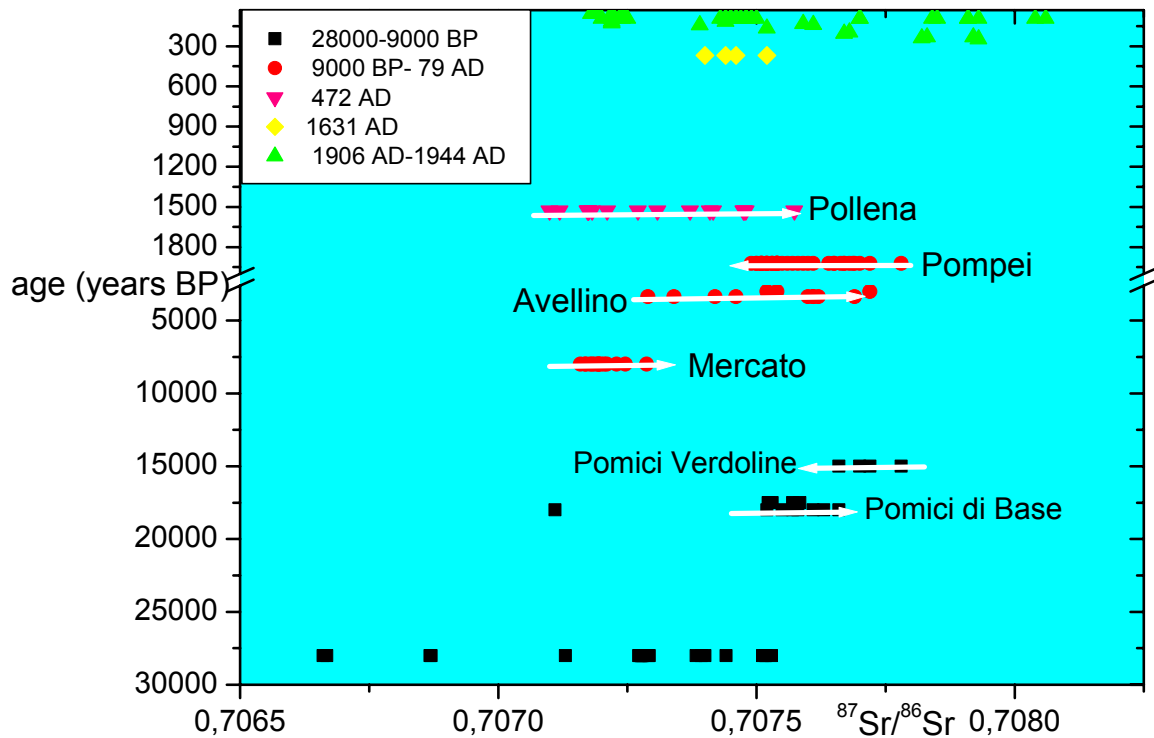


Figure 1. Sr isotopic ratio versus age of eruption of Plinian, subPlinian and strombolian activity. The arrows indicate the variation in isotopes observed during the course of the eruption.

REFERENCES.

Aulinas, M., Civetta, L., Di Vito, M.A., Orsi, G., Gimero, D., in preparation. The Mercato eruption (8ka): eruption dynamics and magma chamber processes.

de Lorenzo S., Civetta L., D'Antonio M., Di Renzo V., Gasparini P., in preparation, The Vesuvius magma chamber: thermal modelling and differentiation processes.

Di Renzo V., Di Vito M.A., Arienzo I., Carandente A., Civetta L., D'Antonio M., Giordano F., Orsi G., Tonarini S., 2005, Magmatic history of Somma-Vesuvius on the basis of new geochemical and isotopic data from a deep bore hole (Camaldoli della Torre). *J. Volcanol. Geotherm. Res.*, in revision

Font, L., Civetta, L., Di Vito, M. A., Orsi, G., in preparation. Geochemistry and petrology of 472AD sub-Plinian vesuvian eruption: insights into shallow magma chamber dynamics.

What kind of matter is this magma anyway?

P. Dellino¹, I. Sonder², R. Buettner² and B. Zimanowski²

¹Centro Interdipartimentale per il Rischio sismico e vulcanico, Università di Bari

²Physical Volcanology laboratory, Wuerzburg University, Germany

Assuming a magma chamber exists under a volcano, and assuming that this magma chamber has a significant amount of hot melt in it, we are actually interested in the material properties of this melt. In particular, by a volcanological point of view, we have interest in the mechanical properties that define the magma behaviour near and during eruptive conditions. By eruptive conditions we define the set of physical realizations that allows for magma movement either from the magma chamber to the volcanic conduit, and from the volcanic conduit out of the crater. Ignoring for now the conditions that lead either to effusive or explosive dynamics, the way in which the melt responds to a stress applied to it is of fundamental importance for describing magma dynamics. A certain shear stress applied on a physical matter will result in a certain deformation of the matter depending on the particular physical state of this matter during application of the stress. As cumbersome and vague as the former sentence might appear, there is not an easier way at looking at the problem, and this is reflected by the fact that for real substances a theoretical way for predicting the expected deformation after the application of a stress does not exist. Empirical relationships are needed to specifically assess the stress-strain relationship of the matter under consideration. Only for very simple monoatomic gases a linear relationship between the stress and strain rate is demonstrated by kinetic theory and successfully applied in fluid-dynamics. This gives way to the well known Navier-stokes equations of fluid physics and viscosity coefficients are consequently defined as the phenomenological relationship between the stress and the strain-rate tensors.

So, if one can assume that the substance of interest has a Newtonian behaviour, the viscosity coefficients can be used for predicting the deformation rate, and hence the velocity field of the substance under the applied stress.

For liquids there is not universal applicability of the Newtonian assumption and experiments are needed to find the stress-strain relationship. Liquids, in facts, hardly can be defined as Newtonian, for example blood is indeed a non Newtonian substance. If by experiments the Newtonian assumption does not hold, different constitutive equations need to be found. It is certainly at this basic stage that rheology plays a fundamental role in constraining magma behaviour .

What about magma?

There is good agreement on the temperature dependence of the stress-strain rate relationship for magmas: for attaining a certain deformation rate a higher stress is needed as temperature decreases.

There is also quite good agreement on the influence of magma composition: the more silica rich the melt the higher the stress needed to reach a certain value of strain rate.

A Newtonian behaviour is generally assumed for magmas at high temperature and with low silica contents and for magmas at lower temperature and higher silica content a plastic (Bingham) behaviour is postulated, where a certain threshold stress is needed for having deformation. Over this threshold, called yield strength, the melt has a behaviour similar to a Newtonian one. Unfortunately there is not much data about the yield strength to be considered, in fact viscometry data on the behaviour of magmas at different shear stress are practically not existing.

The problem of having good empirical data on a wide range of stress-strain rate of magmas have precluded up to now the possibility of the verification of the assumption of Newtonian or Bingham behaviour. This is due to the fact that, casue of the very complex structure of magmas, which can contain bubbles and crystals, specifically designed wide-gap rotational viscometers working in temperature ranges of a few hundreds of degrees centigrades are needed. These viscometers are very different from the commercial ones, as for example those used in the glass industry.

Only very recently a new design of a wide-gap viscometer, realized by the german partners of this paper, has allowed the obtainment of information of the temperature dependent behaviour of actual magmas under a wide range of stress and strain rate condition. This new design allows the obtainment of stress-strain relationship in which the rheological behaviour is not assumed, but verified by experimental data.

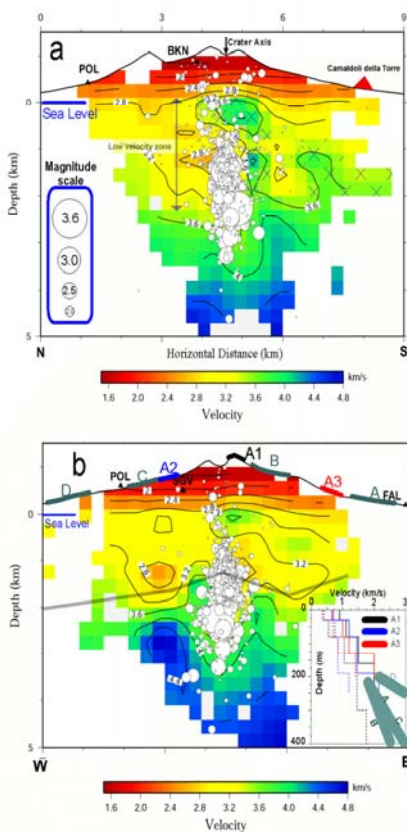
The bad news is that from the very first data it is clear that even low silica high temperature melts have a marked non Newtonian behaviour. The good news is that the stress strain-rate relationship is a power law and that the temperature dependence on the rheological behaviour is well predicted by an exponential function.

It is in our opinion now a good time to start such a kind of investigation also on Vesuvius magmas, for checking their true rheological behaviour and write specifically tailored constitutive equations. The aim is to obtain models for describing the movement of magma from the magma chamber to the conduit and from the conduit to the vent, with the belief that the rheological behaviour can also draw a new picture on the physical state of the melt at the onset of fragmentation of explosive eruptions.

Seismological techniques for the detection of magma chambers
 Edoardo Del Pezzo. INGV-OV.

Velocity, attenuation and scattering tomography are the seismological methods for imaging the geological structures under active volcanoes. In this presentation I want discuss about the uncertainty on data(observables), the physical meaning of the inverted parameters, the resolution, and to show the preliminary applications to Mt. Vesuvius.

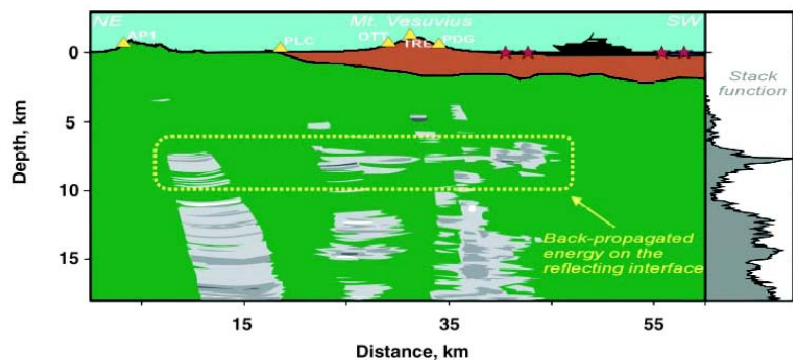
Seismic tomography in general is based on the concept that the (seismic) energy radiated through the geological structures by earthquakes or shots, contains information about these structures that can be retrieved through mathematical methods of optimization. There are three kinds of tomography: velocity, attenuation and scattering tomography. Velocity tomography was firstly introduced in seismology in 1976 by Aki and co-workers (MIT-USA) and by Crosson (Univ. of Washington-Seattle). This tomography is based on the measure of the travel time for all the station-source pairs, that theoretically represents an estimate of the line integral of slowness along the ray connecting receiver and source. After discretization, the problem is solved iteratively starting from an initial slowness structure. The uncertainty on data (observables) is generally of the order of 0.02s for P-wave tomography and one order of magnitude more (depending on the signal-to-noise ratio) for S-waves. The final solution depends on the initial model (stability) and on the data set (robustness). Generally the resolution is empirically achieved by means of tests (checkerboard or other) Intrinsic resolution of the method is determined by the wavelength of the seismic radiation, which furnishes a lower limit to the minimum resolution cell. In case of passive tomography using small magnitude earthquakes, this can be as small as 500m. Velocity tomography yields an image of P and S-wave velocity distribution in the earth volume investigated.



Several thousands waveforms selected on the base of their quality allowed a detailed tomography.

Image of the upper 5 km of the crust (Scarpa et al. 2002).

No magma chambers are clearly visible.

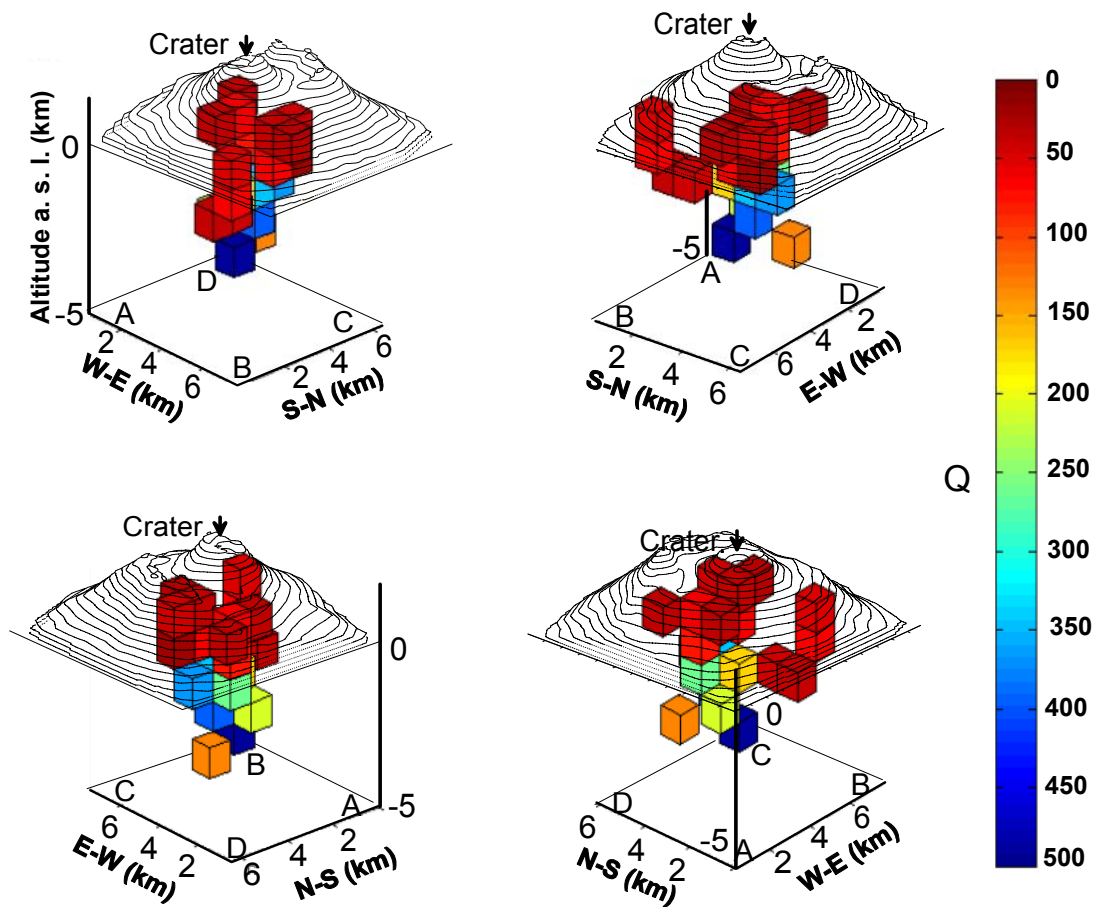


A sill located at 8 km of depth (Auger et al., 2001) is evidenced by a regional tomography based on data from shots



For Mt. Vesuvius, the results are synthesized in the above slide.

Attenuation tomography is based on the observation of the Energy of the seismic waves, that is attenuated by rocks positioned along the ray-path. Also in this case the problem can be discretized and the attenuation parameter for each cell of the discretized volume can be inverted with a mathematical optimization method. Resolution is determined by the minimum wavelength associated to input data, of the order of 500m as in the case of velocity tomography. Inversion is linear, but the uncertainty associated with the observation of seismic Energy is greater than that for travel times. This produces a minimum resolution cell dimension greater than that for velocity tomography, of the order of 1 km. Results for Mt. Vesuvius are preliminary at now, and are shown in the slide reported here below.



Scattering tomography is based on the observation of coda wave energy. From the deviation of the coda decay from a theoretical negative exponential function which represents the scattering model it is possible to invert for the position of the elastic scatterers in space. Scatterers are geological objects with a high contrast in the elastic parameters respect to the average in the investigated volume. This kind of imaging complements the other two, and can help in the interpretation of the attenuation tomography as it may give constraints about the seismic attenuation mechanism. Partial results for Mt. Vesuvius are published by La Rocca et al. (2001). A new study is in progress.

Bibliografia

Scarpa, R., Tronca, F., Bianco, F., Del Pezzo, E. (2002) - High resolution velocity structure beneath Mt. Vesuvius from seismic array data. *GRL*, 29, 21, 10129/2002GL015576.

La Rocca, M., Del Pezzo, E., Simini, M., Scarpa, R., De Luca, G. (2001) Array analysis of seismograms from explosive sources: evidence for surface waves scattered at the main topographical features. *Bull. Seism. Soc. Am.* 91, 2 219-231.

The 1723, 1794, 1822, 1872, 1906 and 1944 eruptions were the most intense (VEI 2-3) over the 1637–1944 period of activity. These eruptions, characterized by mixed effusive-explosive dynamics, always start with lava effusions followed by abrupt transitions to explosive phases: lava fountains, steady columns and occasionally phreatomagmatic activity. The explosive phases have a hawaiian/strombolian up to subplinian style (Arrighi et al., 2001) and are characterized by the deposition of widely dispersed lapilli and ash fallout layers. Systematic sampling of the explosive products emplaced during the most energetic lava fountains of these eruptions, reveals the presence of Mg-rich crystals (olivine and diopside). The phenocrysts present in pyroclastic deposits can be ascribed to two paragenesis in equilibrium with K-phonotephritic and K-tephritic magmas, respectively: a) leucite + salite + Fe-rich olivine ± plagioclase ± biotite and b) Mg-rich olivine, diopside and Cr-spinel included in Mg-rich olivine. Silicate melt inclusions (MI) were analysed in olivine, salite and leucite of the different eruptions. The total volatile content (H_2O , CO_2 , Cl, S) of Lc- and salite-hosted MI is low (<1.5wt%) compared with that of olivine-hosted MI ($H_2O+CO_2+Cl+S+F \sim 5\%$ wt). Assuming saturation conditions for trapped melts, the amount of volatiles (H_2O and CO_2) dissolved in MI provides an estimate of the minimum pressures of melt entrapment using solubility models (Dixon, 1997; Newman and Lowenstern, 2002). The calculated minimum pressure of saturation for olivine-hosted MI ranges between 200 and 400 MPa (Fig. 1), as reported by Marianelli et al. (2005). These are significantly higher than those estimated from K-tephriphonolitic volatile-poor MI from salite and leucite (10-60 MPa). The estimated saturation pressures would correspond to depths ≥ 8 km for MI in olivine and to depths <2km for salite and leucite MI, assuming an average (volcanic, sedimentary silico-clastic and carbonate) rock density of 2600 kg.m^{-3} .

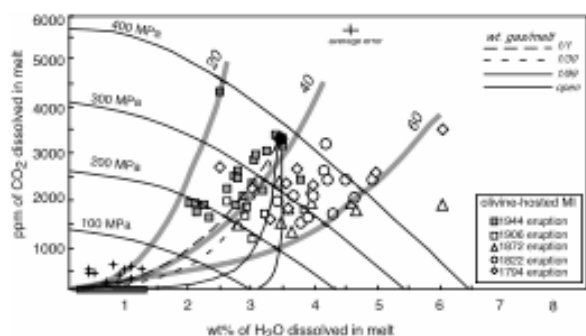


Figure 1. Isobars (100 to 400 MPa) for dissolved H_2O and CO_2 in melt inclusions estimated from Newman and Lowenstern [2002] assuming 45wt% SiO_2 as deduced from the coefficient P_i ($P_i = 1.2$), calculated following Dixon [1997]. For comparison we report also volatile-poor melt inclusions in crystals (salite and leucite) from effusive and weakly explosive events of modern activity of Vesuvius, as shown in the lower left corner of the plot (crosses: data from Marianelli et al., 1999; dark bars: CO_2 not determined). Gray curves: isopleths of constant vapor composition (20, 40, 60 mol% of H_2O) representing the range in CO_2/H_2O of the external gas that is required to generate the data arrays for the different samples. Black dot (initial melt with 3.4 wt% H_2O and 3150 ppm CO_2 at $T=1200^\circ C$) evolve along different paths depending on mass fraction of buffering gas that is present. Calculation based on VolatileCalc (Newman and Lowenstern, 2002).

These MI data demonstrated that the two mineral assemblages are related to crystallization of magmas at different depths. In particular, these data testify for the 1723, 1794, 1822, 1872, 1906 and 1944 eruptions of Vesuvius, the existence of a complex feeding system consisting of deep storage zones and a shallow reservoir, as already evidenced (Marianelli et al., 1999) for 1944 eruption (Fig. 2).

The absence of relationship between the extent of melt differentiation (CaO/Al_2O_3 in olivine-hosted MI) and the trapping pressures, corroborate the hypothesis of melts arranged in a mush column. In our view, the variability of the MI composition and of their saturation pressures implies that the Vesuvius deep feeding system might have been formed by a vertically extended volume of crust containing pockets or interconnected cracks filled by magma at depth > 8 km (Marianelli et al., 2005; Cecchetti et al., 2005). Olivines, formed at different depths and from different melts, were thus entrained and flushed upward by rising magmas.

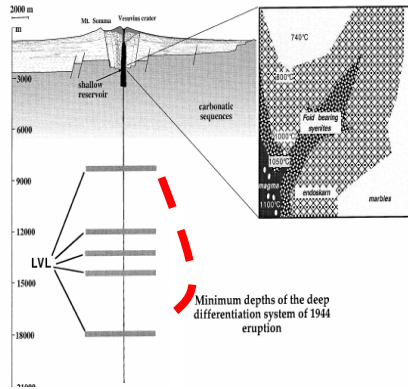


Fig. 2 Sketch for the 1944 feeding system

The Vesuvius shallow magmatic system (<6 km) is hosted within carbonate rocks, and the physical-chemical conditions of magma chambers can be relatively well defined (Cioni et al., 1995, Cioni et al. 1998; Marianelli et al., 1999; Cioni, 2000). Xenoliths from the disruption of magma chamber walls are relatively common in the deposits of Vesuvius eruptions and have been used to reconstruct the magma chamber-wall rock interaction conditions in the different types of chamber. A nearly complete chemical and mineralogical gradation of glass-bearing fergusonites and foid-bearing syenites to salite-bearing clinopyroxenites is observed. The sharp contact, between skarn and foid-bearing syenites (AD 79) or glass-bearing fergusonites (1944) or clinopyroxenites (AD 79, AD 472, 1944), is sometimes seen in collected ejecta. Furthermore, widespread skarn veins are commonly found in several AD 79 marble xenoliths.

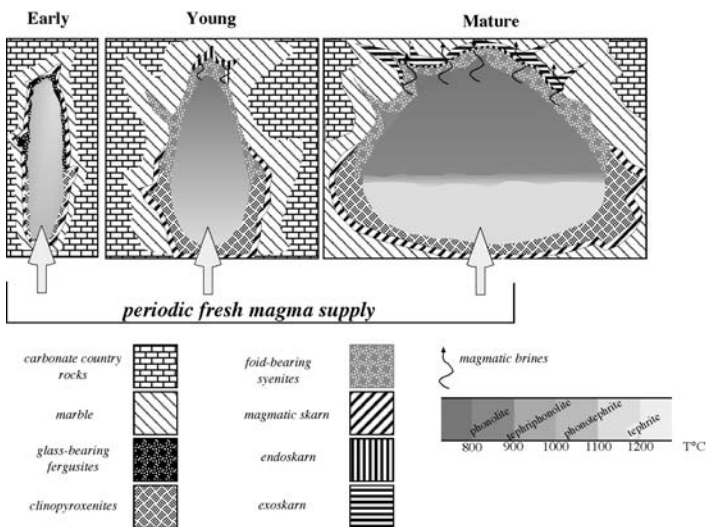


Fig. 3 Sketch of the magma chamber-metasomatic aureole relationships at Vesuvius.

Processes involved in the skarn genesis at the walls of Vesuvian magma chambers are controlled by the characteristics of magma reservoirs (Fulignati et al., 2004). The volatile-phase saturation and exsolution of hypersaline fluid phases from the crystallizing phonolitic upper parts of the “young” (AD 472), and “mature” (AD 79) Vesuvius magma chambers is one of the key processes that strongly constrains the development of the thermometamorphic-metasomatic aureole around the magma chambers (Fig. 3). This is because the exsolved fluid phases are responsible for the transfer of reactants from the chamber into the wall-rock. The infiltration of these fluids, and their interaction with carbonate, represents an effective mechanism for the development of endoskarn (magmatic protolith) and exoskarn (carbonate protolith). Less differentiated, hotter, modified melts, not having exsolved hypersaline fluid phases, promote the generation of magmatic skarn, through melt-solid diffusion processes in the 1944 reservoir, and in the lower and hotter parts of more evolved magma chambers of Vesuvius. In conclusion, the thermal and compositional conditions of Vesuvius magma chambers constrain the type and complexity of their metasomatic aureoles.

References

Arrighi, S., C. Principe, M. Rosi (2001), Violent strombolian and subplinian eruptions at Vesuvius during post-1631 activity, Bull. Volcanol., 63, 126–150.

- Cecchetti A., Marianelli P., Sbrana A. (2005) Input of deep-seated volatile-rich magmas and dynamics of violent strombolian eruptions at Vesuvius. *Development in Volcanology*, in press.
- Cioni, R. (2000). Volatile content and degassing processes in the AD 79 magma chamber at Vesuvius (Italy). *Contrib. Mineral. Petrol.*, 140, 40-54.
- Cioni, R., Civetta, L., Marianelli, P., Metrich, N., Santacroce, R., Sbrana, A. (1995) Compositional layering and syn-eruptive mixing of a periodically refilled shallow magma chamber: the AD 79 Plinian eruption of Vesuvius. *J. Petrol.*, 36, 739-776.
- Cioni, R., Marianelli, P., Santacroce, R. (1998). Thermal and compositional evolution of the shallow magma chambers of Vesuvius: Evidence from pyroxene phenocrysts and melt inclusions. *J. Geophys. Res.*, 103, 18277-18294.
- Dixon, J.E., (1997), Degassing of alkalic basalts, *Am. Mineral.* 82, 368–378.
- Fulignati, P., Marianelli, P., Santacroce, R., Sbrana, A. (2004) Probing the Vesuvius magma chamber-host rock interface through xenoliths. *Geol. Mag.*, 141, 417-428.
- Marianelli, P., N. Metrich, A. Sbrana (1999), Shallow and deep reservoirs involved in magma supply of the 1944 eruption of Vesuvius, *Bull. Volcanol.*, 61, 48–63.
- Marianelli, P., Sbrana, A., Metrich, N., Cecchetti, A. (2005), The deep feeding system of Vesuvius involved in recent violent strombolian eruptions. *Geophys. Res. Lett.*, 32, L02306.
- Newman, S., J. B. Lowenstern (2002), VolatileCalc: a silicate melt-H₂O-CO₂ solution model written in Visual Basic for Excel, *Comp. Geosci.*, 28, 597–604.

Regional and local stresses around magma chambers: an application to Vesuvio, Italy.

Acocella V*, Mattei M., Porreca M., Funiciello R., Massimi E.

Dip. Scienze Geologiche Università Roma Tre. Roma. Italy.

*Corresponding author: acocella@uniroma3.it

The stresses acting at Somma-Vesuvio are the result of the regional (far field) and local (near field) stresses acting in the area.

As far as the regional stresses are concerned, the Tyrrhenian margin of central Italy has undergone Plio-Quaternary extension, developing NW-SE normal faults and NE-SW faults. The NE-SW faults decrease in frequency towards NE with the stretching factor λ , becoming negligible for $\lambda < 1.3$. Plio-Quaternary volcanoes, aligned NW-SE, formed at the intersection among NE-SW and NW-SE faults; fissure eruptions are mostly controlled by NE-SW faults. Structural field data show normal motions for 76% of NW-SE Quaternary faults and transpressive for 73% of NE-SW Quaternary faults. Analogue experiments simulating the NE-SW Tyrrhenian extension show that transverse transpressive faults form with differential extension $\lambda - \lambda_0 > 0.21$. These data suggest that the NE-SW transpressive structures are transfer faults of the NW-SE normal faults, due to relevant differential extension ($\lambda - \lambda_0 > 0.21$) within a stretched crust ($\lambda > 1.3$). The minor dip-slip and strike-slip components of the NE-SW and NW-SE faults respectively, possibly result from the NW-SE extension due to the SE-ward slab retreat beneath the Calabrian arc. The NE-SW and NW-SE extensions in the central-southern Tyrrhenian Sea account for the composite kinematics of the NE-SW structures, which, in turn, exert a two-fold role in controlling volcanism. Where their dip-slip component forms basins, the associated decompression induces magma accumulation (developing central volcanoes) at the intersection among NW-SE and NE-SW systems. Where transfer faults are mainly strike-slip, their inferred subvertical attitude enhances their permeability to magma, accounting for the observed NE-SW fissure eruptions. This seems to correspond to the regional setting of Somma-Vesuvio, where the available geophysical data suggest the presence of a NE-SW trending fault system, interpretable as a major transfer fault, interrupting the continuity of the NW-SE normal faults beneath the Piana Campana. In our model, regional extension, forming NW-SE faults, enhances the overall generation and rise of magma along the margin, but NE-SW structures focus magma rise and emplacement at shallower levels.

As far as the local stresses are concerned, these can be mainly inferred from the dike complex outcropping along the Somma scarp and the 1631-1944 fissure eruptions found on the Vesuvio flanks. The dike complex consists of approximately 100 dikes, mostly radial or subradial, emplaced before than 18 ka. The fissure eruptions are the surface expression of the emplacement of dikes radiating from the cone. Both indicators suggest the existence of a shallower stress field related to the topography of the volcano, which induces local variations in the intensity and orientation of the 3 components of the stress field.

References

- Acocella, V., Salvini, F., Funiciello, R., Faccenna, C., 1999. The role of transfer structures on volcanic activity at Campi Flegrei (Southern Italy). *Journal of Volcanology and Geothermal Research*, 91, 123-139.
- Acocella, V., Funiciello, R., 2002. Transverse structures and volcanic activity along the Tyrrhenian margin of central Italy. *Mem. Soc. Geol. It.*, 1, 739-747.
- Bianco, F., Castellano, M., Milano, G., Ventura, G., Vilardo, G., 1998. *Journal of Volcanology and Geothermal Research*, 82, 199-218.
- Bruno, P.P., Cippitelli, G., Rapolla A., 1998. Seismic study of the Mesozoic carbonate basement around Mt. Somma-Vesuvius, Italy. *Journal of Volcanology and Geothermal Research*, 84, 311-322.
- Bruno, P.P., Rapolla, A., 1999. Study of the sub-surface structure of Somma-Vesuvius (Italy) by seismic reflection data. *Journal of Volcanology and Geothermal Research*, 92, 373-387.
- Cioni, R., Santacroce, R., Sbrana, A., 1999. Pyroclastic deposits as a guide for reconstructing the multi-stage evolution of the Somma-Vesuvius caldera. *Bulletin of Volcanology*, 60, 207-222.
- Marinoni, L.B., Gudmundsson, A., 2000. Dykes, faults and palaeostresses in the Teno and Anaga massifs of Tenerife (Canary Islands). *Journ. Volcanol. & Geoth Res.*, 103: 83-103.
- Marinoni, L., 1995. The Monte Somma scarp: new preliminary stratigraphy and structural insights. *Per. Mineral.*, 64, 219-221.
- Marinoni, L., 2001. Crustal extension from exposed sheet intrusions: review and method proposal. *Journ. Volcanol. & Geoth Res.*, 107: 27-46.
- Santacroce, R., 1987. *Somma Vesuvius*. C.N.R. Rome; 251 pp.
- Scandone R., Giacomelli L., Gasparini P., 1993. Moutn Vesuvius: 2000 Years of volcanological observations, *J.Volcanol. Geoth. Res.*, 58, 4-25.

Ventura, G., Vilardo, G., Bruno, P.P., 1999. The role of flank failure in modifying the shallow plumbing system of volcanoes: an example from Somma-Vesuvius: Italy. *Geophysical Research Letters*, 26, 3681-3684.

Zollo, A., Gasparini, P., Virieux, J., le Meur, H., de Natale, G., Biella, G., Boschi, E., Capitano, P., de Franco, R., dell'Aversana, P., De Matteis, R., Guerra, I., Iannaccone, G., Mirabile, L. Vilardo, G., 1996. Seismic evidence for a low-velocity zone in the upper crust beneath mount Vesuvius. *Science*, 274, 592-594.

Project V3 – Vesuvius

Task 1. The magma feeding system

responsible: Prof. Domenico Patella
Dr. Zaccaria Petrillo
Dr. Ida Diaferia
Dr Maria Giulia Di Giuseppe
Dr. Antonio Troiano
Dr. Boris Di Fiore

INTRODUCTION and something about the MT method

In the last years there has been a remarkable acceleration in the use of electromagnetic methods (EM), applied to the Earth, both for structural scopes and for the reduction of the seismic and volcanic risk; it is worthwhile to remember the project of the USGS which is devoted to acquire by, approximately 50 magnetotelluric (MT) stations in contemporary recording on the San Andreas fault, EM data for purpose of monitoring. In particular the application of methods EM in volcanic environments is argument of strong interest like shows varies literature articles developed in recent years. Given to the tight relation between resistivity (generally the target of the most of EM methods) and some physical characteristics of the volcanic structure, either superficial or deep,

- to molten zones, or partially fused, correspond low values of resistivity of the order of some ohm-m
 - to superficial parts with active hydrothermal systems correspond values comprised between ohm-m and tens of ohm-m
 - to the cold volcanic structure (far from the values of fusion of the rocks) correspond commonly values of resistivities of hundred, thousands and sometimes tens of thousands of ohm-m
- EM methods turns out a powerful tool in the structural reconstruction and in the definition of dynamics of active volcanoes.

The main methodology in order to explore the deep structure is the MT method, the exploration depth varies from tens of meters to tens of km depending on the analyzed frequency; a functional relation exists (in 3-D case extremely complex) that link the depth of surveying to the frequency of EM wave, but in a generalized manner it can be asserted that to high frequency correspond low depths of exploration, with diminishing of the frequency such depth increases. The source of method MT is the variations of EM field of external (to the Earth surface) origin in the band of freq. $10^4 \div 10^{-4}$ Hz (the method works in the space of Fourier),

defines a tensor of rank 2, invariant with time and local $\rho_{ij}(\vec{r} \in surface, \omega)$ (here is not explicit the relation with the distribution of resistivity of the subsoil) with the dimensions of one the complex resistivity. Such tensor in order to have a good MT develop needs some hypotheses.

- the EM incident wave on the Earth surface (MT source) must be uniform; this requirements is too strong, it is sufficient that for every analyzed frequency the portion of surface invested from uniform EM field has a ray of approximately two times the depth of penetration
- the source must be stationary and random polarized.

Under these hypotheses the MT tensor is well definable, it is named far field, and exist many codes to invert (1-D, 2-D and 3-D) the estimate MT's tensor collected on Earth surface. The most codes are based on the Tikhonov's regularization (being not linear the inverse problem in the parameter resistivity and ill-posed) and these allow for the reconstruction of the distribution of resistivity of the subsoil.

The two main search lines in MT regard

- the data inversion; that is the exploration of the space of the models (parametrized) with the condition of search of the minimum of a functional of misfit. Such line of search has not still allowed for an automatization of the data inversion, in part because from the theoretical point of view it still does not exist a demonstration of the 1 to 1 relation between space of the models space of data (it exists in the case 1-D and for 2-D TM mode (Transverse Magnetic), while there are numerical indications for the case 3-D), in part for problems of sampling of MT data on Earth surface only discrete; think that renders highly ill-posed the problem.
- the estimate of the resistivity tensor; in literature from the 70 today an intense development of statistical methods for the estimate of the resistivity can be followed, from the single station based on the minimums square and then on the robust methods that analyzed the detail of the distribution of error, to the remote reference ones that pulled down the incoherent noise substantially, until the multivariate analysis, introduced when more stations MT are become available in contemporary acquisition. Such method, based on the

diagonalization of the covariance matrix, allows an estimation of the coherent noise to the scale of the spatial distribution of the station array and in principle allows for a separation of the contributions of MT field and near field (coherent noise).

STATE OF THE EM RESEARCH AT Mt. SOMMA-VESUVIO

In last the 2 decades the Mt Somma-Vesuvio volcano complex has been explored, amongst the other geophysical methodologies, through the application of EM methods. In particular the use of the MT, integrated with EM controlled source methods (dipole-dipole deep geoelectric, DGS and transient electromagnetic, TEM), has been applied to the Vesuvio from two groups of research, (Di Maio et al. 1998, Manzella et al. 2003). It turns out similar MT curves in shape but with substantial shift. In fig.1(a, b) localizations of stations MT and DGS (Di Maio et al. 1998, upper figure) and localizations of stations MT (Manzella ET al. 2003, lower figure). In figure 2 a comparison of the different estimate of the resistivity obtained from the two groups in contiguous sites; in particular is clear how, the curves show the same development and the conductor (the minimum of the curves) characterized from the two groups is localized to the same frequency (period), while the absolute value is shifted of also two orders of magnitude along all the curves. In the paper of Manzella et al. (2003) TEM surveys were used in order to control the static level of the curves for MT surveys. In the paper of Di Maio et al. (1998) the corrected level of the magnetotelluric curves was instead determined from the comparison with the dipole-dipole geoelectric tomographies. On the other hand in Manzella ET al. (2004) it is discussed, moreover, that MT curves was in agreement with geoelectric tomography NS introduced in Di Maio et al. (1998). Since between the curves of MT resistivity discussed in the two papers are more than a decade shifted (in almost all the soundings) evidently in one of the two cases is an erroneous appraisal of the geoelectric tomography. DGS data set have been subsequently inverted (by Prof. Siniscalchi Agata of the Bari university, personal communication) through the code RES2Dinv (Loke and Barker, 1995). In figure 3 are showed the two sections of resistivity, North-South (a) and East-West (b) obtained by the inversion of DGS's, in which it has been considered the topographic effect. As it can be evinced by a simple inspection of the 2 models of resistivity the average values of the resistive basement are elevated (also of the order of $10^5 \Omega\text{m}$) and substantially in agreement with the superficial part of the model obtained from MT in Di Maio et al.. It exist however still ambiguity elements, as an example TEM gives values of resistivity for the volcanic cover much lower (Manzella et al.) and in clear contrast with DGS (Di Maio et al.), moreover the MT estimators used in both papers were substantially of single station, and for some surveys of remote reference, this has not allowed an estimate of the coherent noise, not being able therefore to exclude effects of near field and therefore source effects.

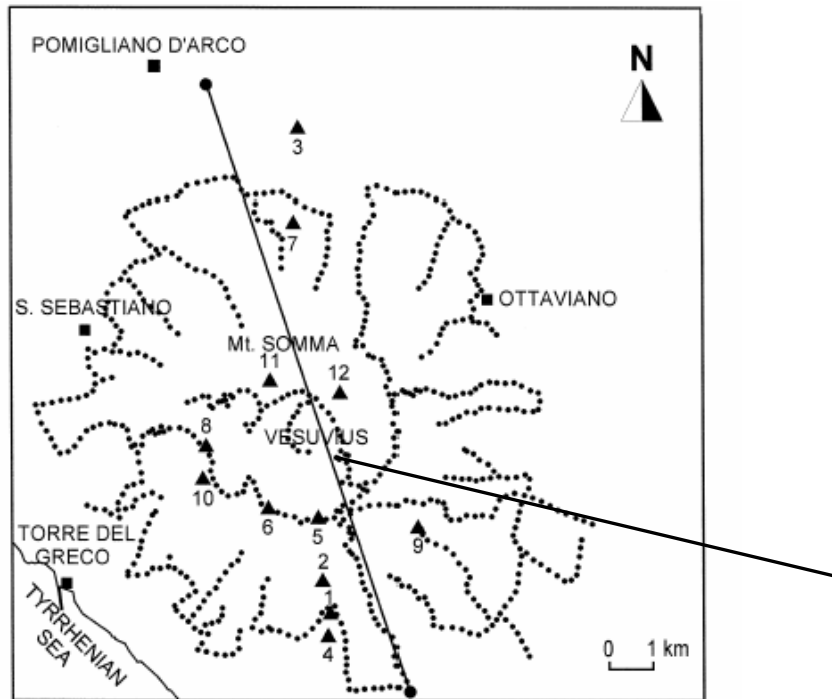


Fig. 1. Geophysical survey location map in the Mount Somma–Vesuvius volcanic area. Dots, full line and triangles indicate the SP mapping circuits, the DG pseudosection profile and the MT sounding stations, respectively.

a)

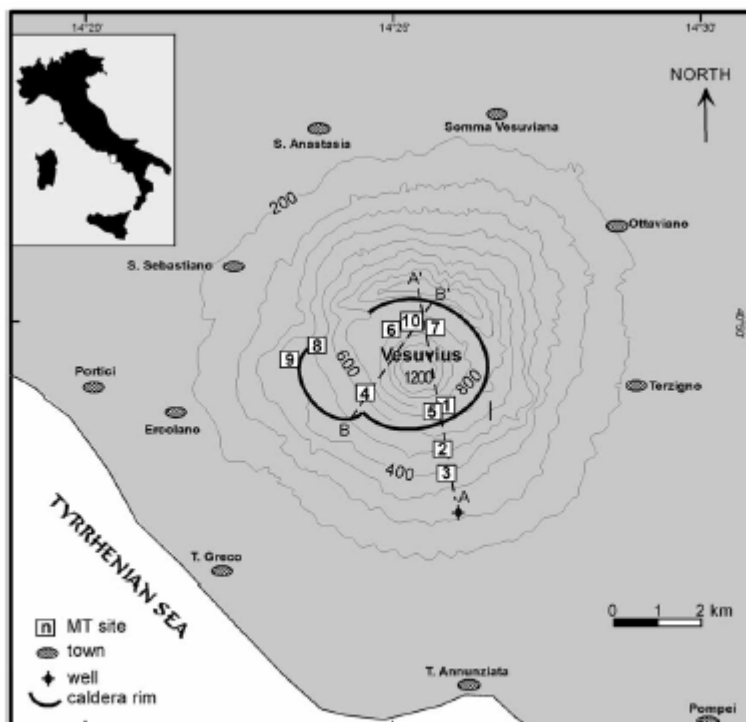


Fig. 1. Location map of the Somma-Vesuvius study area. Preliminary MT soundings to test the hypothesis of shallow versus deep magma chambers are shown. The relative numbers inside white boxes identify sites. The caldera rim and the TreCase well location are also shown. Profiles A-A' and B-B' described in the text are indicated.

b)

Figura.1 Maps of localizations of MT surveys (triangles and squares) and DGS (lines) at Mt. Somma-Vesuvius from Di Maio et al. a) and Manzella et al. b).

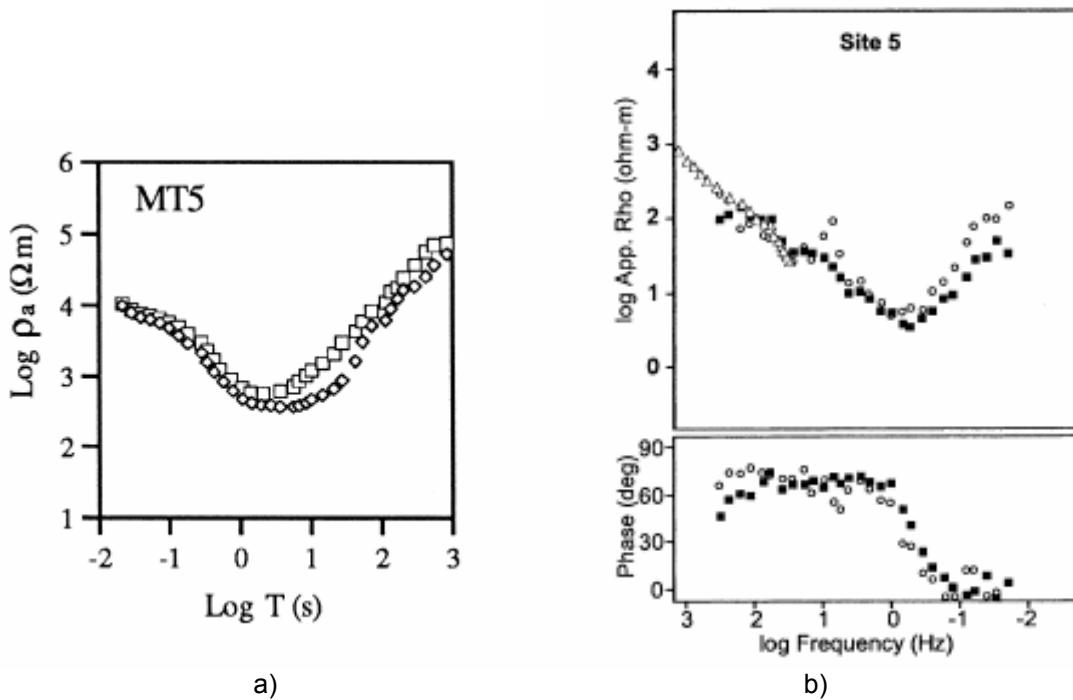
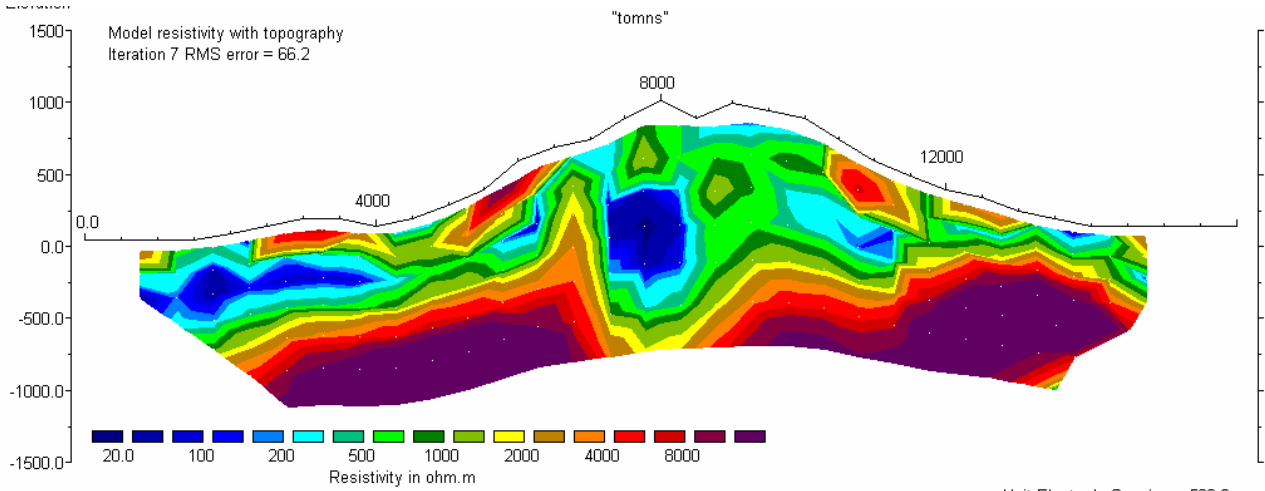
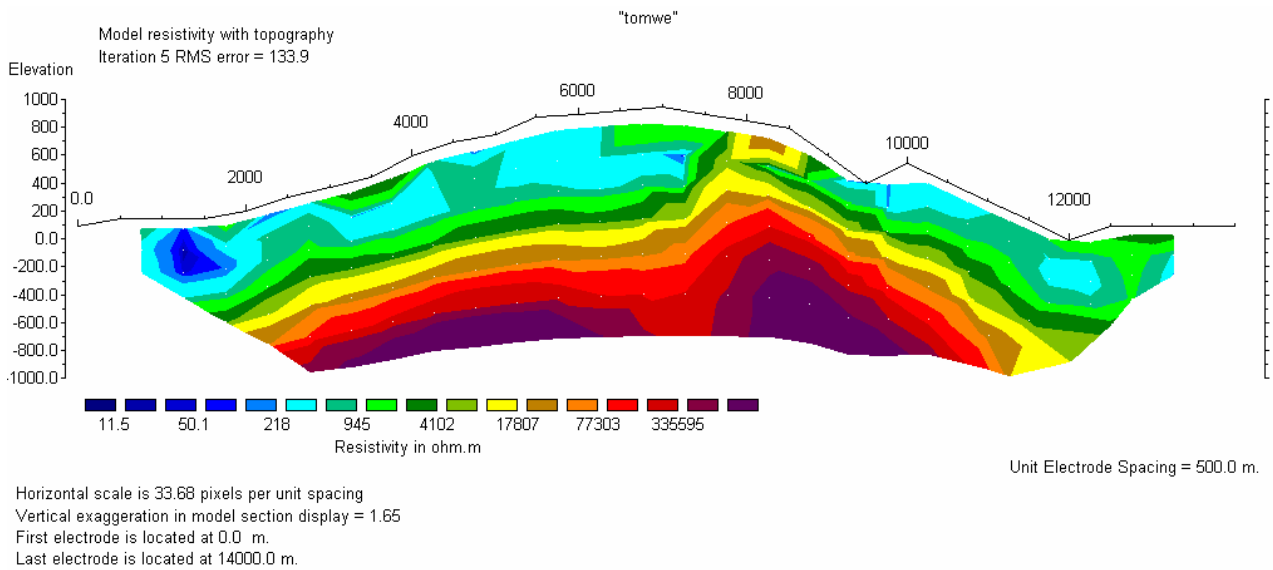


Figure 2. MT Curves in the same site at Mt Somma-Vesuvius obtained by Di Maio et al. a), Manzella et al. b). x axis: log of the frequency, y axis: log of the resistivity. With the Triangles, b), the resistivity obtained with the TEM.



Horizontal scale is 29.13 pixels per unit spacing
 Vertical exaggeration in model section display = 1.97
 First electrode is located at 0.0 m.
 Last electrode is located at 16000.0 m.

a)



b)

Figure 3: electric tomography obtained by the RES2DINV along Nord-Sud a) ed Est-Ovest b) applied to DGS data, see figure 1 for localization. With the colours the values of resistivity

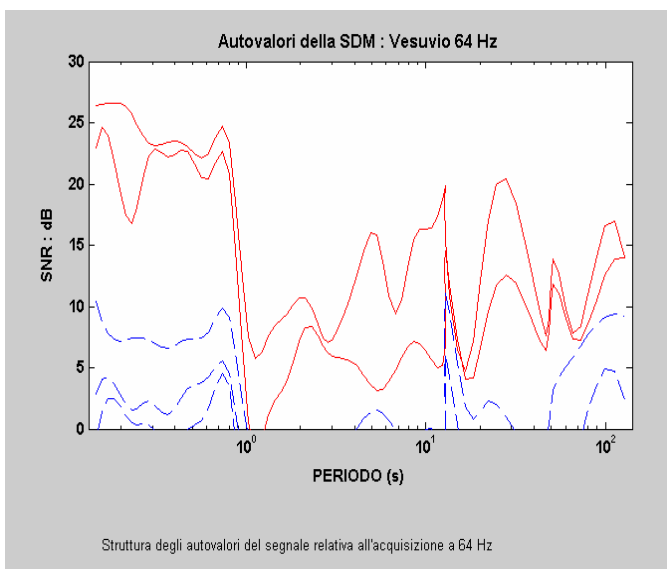
THE PROJECT

The scope of the project is the construction of a detailed 2-D East-West electric image of Torre del Greco fault, substantially along the DGS section of figure 1, a); the estimate depth of exploration will be around 3 km. It will be acquired contemporary MT data by

- 2 MT Metronix stations (24 bit, 6 magnetic channels, 4 electric channels),
- 1 MT station (24 bit, 2 magnetic channels 2 electric channels),
- 1 MT station continuous Array profiling (24 bit, 2 magnetic channels, 8 electric channels),
- 1 magnetic station (21 bit, 3 magnetic channels) used as remote reference.

For the control on the static shift it will be carried, in the same MT sites, CSAMT (Control Source Audio Magnetotelluric) surveys, the latter uses 2 magnetic orthogonal sources of artificial EM field in the high

frequency band ($10^5 \div 10^{-3}$ Hz) in order to estimate correctly the resistivity tensor. Data will be processed by RMEV (Robust Multi-Variate Error in Variables, Egbert 1998) code, given the nature highly multi-variate of the acquired data (27 contemporary channels). The multi-variate technique has been experimented at Vesuvio by means of two contemporary MT stations in order to explore the length of correlation of the MT signals, preliminary results have shown a good signal/noise ratio (estimated by data covariance matrix) and a good level of coherence between the two sites distant approximately 4 Km, fig. 4.



In the fig.4 a) the eigen-values of the spectral density matrix relative to a 64 Hz acquisition in two sites at Vesuvio distant some km and carried out with two

stations MT with 3 magnetic channels and two electric channels. X axis, the period in second, y axis the Signal/Noise ratio expressed in $10\log(S/N)$. It is clear how the average S/N ratio for the first 2 eigen-values (red line) is at least 10, confirming the presence at least two coherent sources of field EM in the entire explored band.

Figure 4 a)

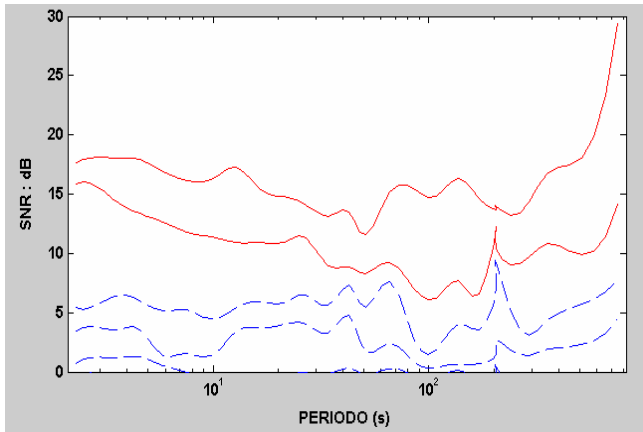


Figure 4 b)

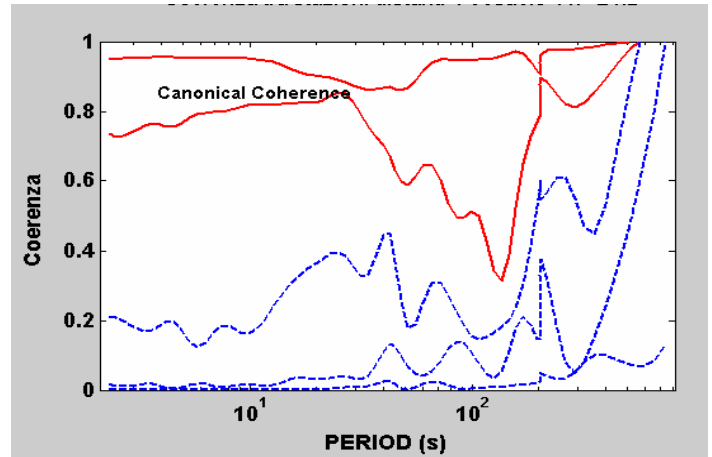


Figure 4 c)

In figure 4 b) is showed the eigen-values structure relative to 2 Hz acquisition, and relative to 4 hours record, in figure 4 c) the canonical coherency between the two stations.

The project will provide, as initial phase, the separation of the contributions of near fields from those of far field. It will be inverted the only far field contributions. By means of MT resistivity tensor estimate, a 2-D model will be obtained by a not linear inverse code based on the conjugates gradient (Rodi and Mackie, 2001), constrained by DGS (East-West, fig.1) tomography.

The first year provide the acquisition of MT and CSAMT data along a line passing to south of the crater and long 3÷4 km

The second year provide the elaboration and the inversion of MT far field resistivity tensor.

BIBLIOGRAPHY

Di Maio, R., Mauriello, P., Patella, D., Petrillo, Z., Piscitelli, S., Siniscalchi, A., 1998. Electric and electromagnetic outline of the Mount Somma-Vesuvius structural setting. *J. Volcanol. Geotherm. Res.* 82, 219-238

Egbert, G. D., 1997, Robust multiple station magnetotelluric data processing: *Geophys. J. Internat.*, 130, 475-496.

Loke, M. H. and Barker, R. D., 1995. Least-squares deconvolution of apparent resistivity pseudosections. *Geophysics*. Vol. 60, No. 6; P. 1682-1690.

Manzella, A., Volpi, G., Zaja, A., Meju, M., 2004. Combined TEM-MT investigation of shallow-depth resistivity structure of Mt Somma-Vesuvius, *Journal of Volcanology and Geothermal Research* 131, 19-32

Rodi, W., Mackie, R.L., 2000. Nonlinear conjugate gradients algorithm for 2-D magnetotelluric inversion. *Geophysics* 66, 174-187.

PHYSICAL CONDITIONS OF PRIMITIVE BASALTIC AND TEPHRITIC MAGMAS FROM VESUVIUS: EXPERIMENTAL CONSTRAINTS

M. Pichavant, B. Scaillet and A. Pommier

Institut des Sciences de la Terre d'Orléans, UMR CNRS 6113, Orléans, France

Experiments on primitive Vesuvius lavas have been performed to answer to the following questions: (1) what are the physical conditions (P, T, volatile fugacities, fO_2) of primitive Vesuvius melts ? (2) what is the significance of melt inclusion compositions ? (3) what is the composition of mafic magma batches and (4) what is the structure of the feeding system beneath Vesuvius ?

Two samples were investigated: a tephrite (VES-9: 48% SiO_2 , $Na_2O+K_2O=7.35\%$, 6.73% MgO, $CaO/Al_2O_3=0.88$) from a subplinian 8th century eruption, and a K-basalt (VS96-54A: 48% SiO_2 , $Na_2O+K_2O=5.83\%$, 7.97% MgO, $CaO/Al_2O_3=1.04$) from the open-conduit 1944 eruption. VES-9 is more mafic than the compositions investigated by Dolfi and Trigila (1978) and Trigila and De Benedetti (1993). VS96-54A has a MgO concentration higher than VES-9, approaching the composition of the most primitive inclusions from the 1631-1944 period (Marianelli et al., 1995; 1999; 2005). The high CaO concentration (13.96 wt%) and CaO/Al_2O_3 (1.04) reflects the porphyritic, probably partially cumulative, nature of this sample.

Both 1 atm and high pressure experiments were performed from glass starting materials. Experiments at 1 atm were carried out in a vertical gas-mixing furnace using the wire-loop method. The high pressure experiments were conducted systematically between 0.5 and 2 kbar and 1000 and 1200°C in an IHPV fitted with a drop-quench device and pressurized with Ar-H₂ for control of fO_2 . The main experimental parameter was the H₂O content of the melt. A few experiments were performed with H₂O-CO₂ mixtures. Others were carried out with olivine added, to force olivine saturation. Charges were studied by SEM and analyzed by electron microprobe, Karl-Fischer titration and FTIR .

Several essential aspects of Vesuvius primitive melts are successfully simulated by these experiments: (1) phase equilibria and conditions of crystallization of Vesuvius magmas (liquidus Cpx, Lc restricted to melt H₂O < ca. 1 wt%, Phl to > 5 wt%); (2) clinopyroxene and melt compositions (in agreement with phenocrysts and evolved melt inclusions); (3) H₂O and CO₂ concentrations in a melt cosaturated with Fo₉₁ Ol and Mg#91 Cpx at 1150°C, 2 kbar are 2.94 wt% and 2268 ppm (identical to the average of the volatile concentrations analyzed in melt inclusions of the 1631-1944 period, Figure 1). However, olivine was found in only one charge and is on the liquidus neither for VS96-54A nor for VES9. This, and the fact that the most primitive melt compositions of the 1631-1944 period are not reproduced experimentally raises questions about the representativity of the starting compositions used.

Olivine-added experiments allow the Ol+ Cpx cotectic to be located for primitive Vesuvius magmas. It is shown that the two starting compositions plot in the Cpx primary field, consistent with their determined crystallization sequences. Comparison between melts from olivine-added experiments and melt inclusions show that the most primitive trapped Ol- (but not Cpx-) saturated melts between 1150 and 1200°C. These primitive inclusions preserve evidence for an early Ol crystallization stage in Vesuvius magmas, followed by cotectic Ol + Cpx and then Cpx. This Ol crystallization stage is not recorded in the composition of erupted lavas which are undersaturated in Ol. The paradox may be explained either by magma mixing with Cpx-rich differentiates or by magma interaction with carbonate rocks.

These results suggest a new model for the magma feeding system beneath Vesuvius. The 1631-1944 period is dominated by the ascension of K-basalt magma batches from the upper mantle to levels of 2-3 km, which corresponds to the depth of the phonotephritic crystal mush tapped by recent (eg, 1944) eruptions. Limited Ol crystallization occurs during ascent in small sill-like bodies located at depths around 8 km, possibly in relation with a structural discontinuity level which promotes interaction between magma and carbonate rocks. Transition to a regime characterized by growth of a magma reservoir requires a reduction of the flux of K-basalt batches, which induces cooling and differentiation towards tephriphonolitic and phonolitic compositions.

References

- Dolfi D, Trigila R (1978), *Contrib. Mineral. Petrol.*, 67, 297-304.
Marianelli P, Metrich N, Santacroce R, Sbrana A (1995), *Contrib. Mineral. Petrol.*, 120, 159-169.
Marianelli P, Metrich N, Sbrana A (1999), *Bull. Volcanol.*, 61, 48-63.
Marianelli P, Sbrana A, Metrich N, Cecchetti A (2005), *Geophys. Res. Lett.*, 32, L02306.
- Trigila R, De Benedetti AA (1993), *J. Volcanol. Geotherm. Res.*, 58, 315-343.

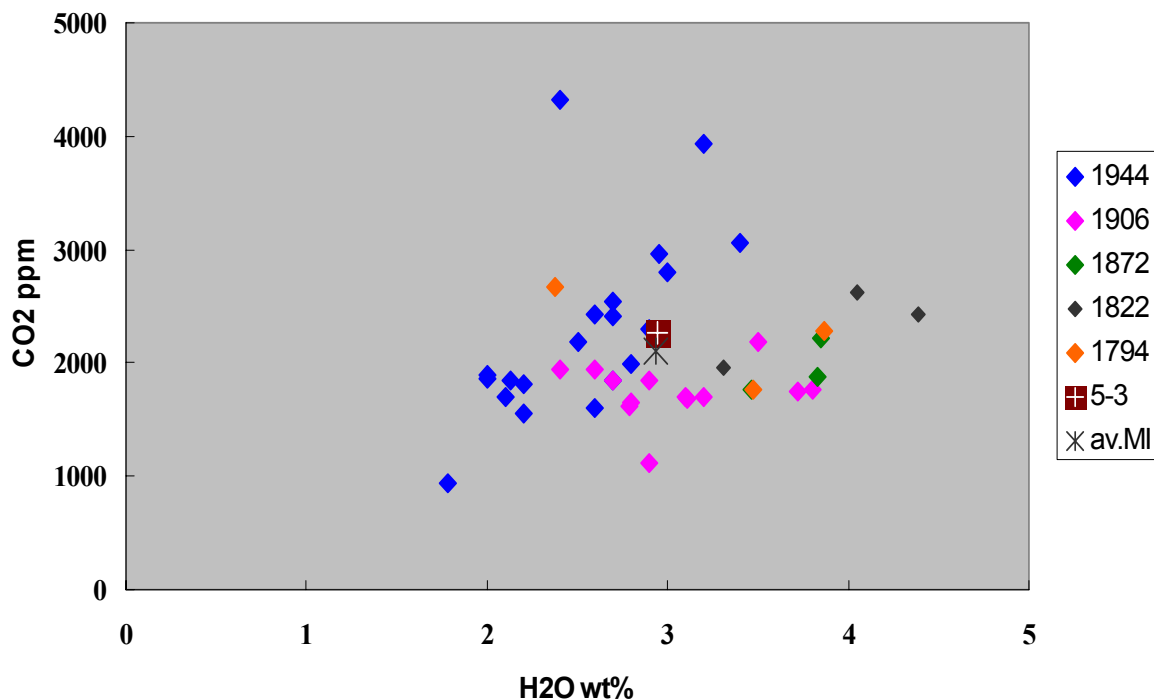


Figure 1. H₂O and CO₂ concentrations in glass inclusions from the 1631-1944 period (Marianelli et al., 1995, 1999, 2005) compared with concentrations in an experimental melt cosaturated with Fo₉₁ Ol and Mg#91 Cpx at 1150°C, 2 kbar (# 5-3). The experimental concentrations practically coincide with the average for all melt inclusions (av. MI) which suggest an average pressure of trapping of 2 kbar for the melt inclusions.

Aspects that need further experimental work or methodological developments to improve volcanic hazards assessment at Vesuvius.

B. Scaillet and M. Pichavant.

The experimental results so far obtained on Vesuvius magmas suggest the following guidelines for future work.

1. Given the apparent pressure decrease documented for storage conditions at Vesuvius (Fig. 1), it is of utmost importance that additional key events that occurred before and after the period covered by presently done experiments (Pollena to Mercato eruptions) be tackled using an experimental approach in order to confirm this trend. Following discussions at Roma and Napoli, it appears that those key eruptions are the 1631, Pomici di Base and possibly Greenish eruptions. For each of these, combined detailed petrological and experimental work (phase equilibria) need to be carried out on representative rock specimens, carefully selected on the field. A field campaign towards this end will be done in the next weeks.
2. The preliminary volatile analyses of selected run products obtained on phonotephrite and tephrite experiments done with mixed volatiles (H_2O and CO_2) show that current solubility models strongly underestimate the CO_2 content of tephritic melts. We estimate that the main level of magma ponding beneath Vesuvius is around 200 MPa, and not in the range 300-600 MPa, as previously suggested. However, unravelling rigorously the barometric information of melt inclusions at Vesuvius demands that the volatile solubility laws of Vesuvius magmas be explicitly calibrated using laboratory experiments. This is currently achieved within the framework of the PhD thesis of Priscille Lesne, done at ISTO, with funding for experiments from the on-going programma quadro of INGV. Determining the solubility laws of main volatile species of Vesuvius magmas is also central for a realistic numerical simulation of degassing process during magma uprise. Numerical simulation of magma degassing, with emphasis on the evolution of gas composition, is likely to supply vital information as to the type of surface gas composition to be expected in case of volcano unrest.
3. Following discussions held at the Roma meeting, it appears that considerable uncertainties still surround the physical properties of Vesuvius magmas. We are currently setting up one internally heated vessel to perform conductivity measurements of magmas at high P and T (project leader Fabrice Gaillard), that will be operative in the next months. In the mid term (1-2 years), we plan to do also seismic measurements on partially molten material. We believe that measurement of either resistivity or seismic properties of Vesuvius magmas under P-T- H_2O - fO_2 conditions as defined by our on-going phase equilibrium work, is likely to greatly help geophysicists to deconvolute the various signals they measure at Vesuvius. This target was not proposed in the original project because we were still uncertain as to the schedule of equipment acquisition. This step is over now, and we propose to carry on at least preliminary measurements, as soon as the set up will be ready, and if the geophysical community is interested.

Phase equilibrium constraints on pre-eruption conditions of Plinian and sub-Plinian events at Vesuvius

B. Scaillet¹, M. Pichavant¹, R. Cioni², A. Sbrana³ P. Marianelli³

¹Institut des Sciences de la Terre, UMR 6113, CNRS-UO, 1a rue de la Férollerie, 45071 Orléans, cedex 2, France

²Dipartimento di Scienze della Terra, Via Trentino 51, 09127 Cagliari, Italy

³Dipartimento di Scienze della Terra, Università di Pisa, Italy.

We have worked out the phase relationships of various eruptive events, representative of explosive eruptions having occurred over the past 8000 years. The prime aim is to constrain the pre-eruption conditions of such explosive events as well as their possible variations with time.

The selected starting materials are four representative phonolites of Vesuvius, corresponding to the most evolved magmas of Mercato (8010 B.P.), Avellino (3360 B.P.), Pompei (A.D. 79) and Pollena (A.D. 472) eruptions, which are assumed to correspond to the topmost portion of the tapped reservoir(s). In addition, we have investigated the phase equilibria of the Pollena tephriphonolite, which corresponds to the most mafic magma erupted during that event, and which is assumed to represent to bottom part of the emptied reservoir. Phase relationships have been established via hydrothermal experiments. Crystallisation experiments on phonolites have been performed in the pressure range 100-300 MPa, at temperatures from 775 to 950°C, melt water contents from 1 to 8 wt%, fO_2 kept in the range NNO-NNO+1, and for variable fluid phase compositions. Complete polythermal-isobaric sections at 200 MPa, polybaric-isothermal sections at 800°C and 775°C have been established for each composition. A similar strategy was followed for the mafic Pollena but we varied P between 50 to 200 MPa, and T between 950 to 1050°C.

The comparison between experimental run products and phenocryst assemblages of phonolites allows us to place tight constraints on pre-eruptive conditions of Plinian to sub-Plinian eruptions at Vesuvius. Pre-eruptive temperatures are always close to $800 \pm 15^\circ\text{C}$, whilst melt H_2O contents show considerable variations from near saturation at 200 MPa (7 wt% dissolved H_2O) down to 4 wt%. The reservoir that fed Plinian phonolitic eruptions (Mercato, Avellino and Pompei) is located at 200 ± 20 MPa whilst that of the Pollena event is estimated to be at 90-100 MPa. Phase equilibria of the the mafic Pollena show little variations in the range 50 to 200 MPa, being dominated by the crystallisation of clinopyroxene, leucite and phlogopite, the latter under H_2O -rich conditions only. In contrast, melt compositions show clearly that the mafic Pollena cannot produce the Pollena phonolite at a pressure of 50 MPa, since leucite fractionation prevents the residual liquids from being as rich in K_2O as the Pollena phonolite. This provides thus a minimum pressure for the Pollena reservoir. In general, leucite widespread occurrence in Vesuvius tephriphonolites appears to be mostly related to decompression crystallisation. Liquid lines of descent produced at either 100 or 200 MPa perfectly reproduce the observed bulk rock compositions sampled by the Pollena event, suggesting that crystal fractionation is the dominant mechanism of shallow magma evolution. These experiments are unable, however, to reproduce Pompei or Avellino type phonolites, suggesting that the magma feeding system changed between Pollena and Pompei. Altogether, the experiments evidence that storage conditions have changed between Pompei and Pollena eruptions, with an upward migration of about 100 MPa. The cause of such a migration is unknown, but could be due to changes in the shape/volume of the volcanic edifice following Plinian decapitation during the Pompei event.

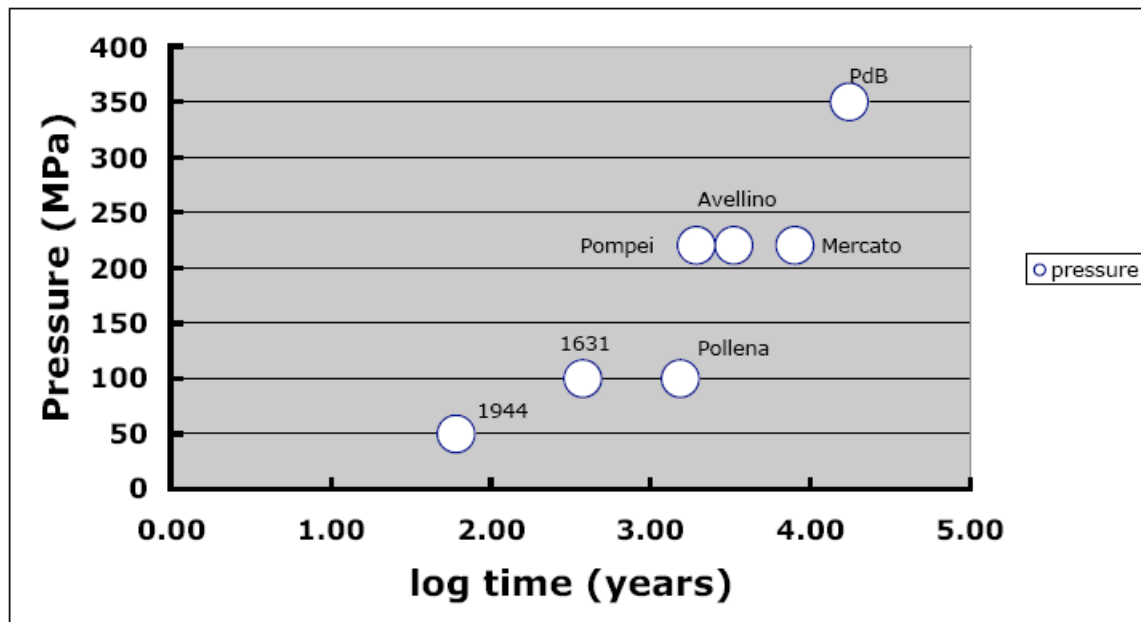


Figure 1 : Evolution of the pressure of magma storage at Vesuvius with time. Data for the Pomici di Base (PdB) is from Landi et al . (1999) : for 1944 from Fulignati et al. (2003). The pressure of the 1631 event is inferred.

When considering the barometric data available for other Vesuvius events (Landi et al., 1999 ; Fulignati et al., 2003) it appears that, since the Pomici di Base eruption, the crustal reservoir has migrated toward shallower levels (Fig. 1). The apparent temporal trend needs, however, to be confirmed via either detailed petrological studies of key eruptions (e.g. 1631) or via the acquisition of additional phase equilibrium data of older explosive events (e.g. Pomici di Base)

References

- Landi, P., Bertagnini, A., Rosi, M. 1999. Chemical zoning and crystallisation mechanisms in the magma chamber of the Pomici di Base plinian eruption. *Contrib. Mineral. Petrol.* 135, 179-197.
- Fulignati, P., Marianelli, P., Métrich, N., Santacroce, R., Sbrana, A. 2003. Towards a reconstruction of the magmatic feeding system of the 1944 eruption of Mt Vesuvius. *J. Volcanol. Geotherm. Res.* 3106, 1-10.

Magma ascent, precursors and eruption dynamics at Mt St Helens between 1980 and 2004

R. Scandone, F. Fattori Speranza, L. Giacomelli

Dipartimento di Fisica, Università Roma Tre
Via Vasca Navale 84, 00146, Roma, Italy

On March 20, 1980, Mt St Helens entered a period of unrest, which resulted in a sector collapse of the volcano with a lateral blast and a plinian eruption, followed by six years of episodic eruptions. The entire eruptive period can be subdivided into different stages (Scandone et al, in preparation).

- 1- Precursory stage and early magma ascent: 20-27 March 1980
- 2- Cryptodome intrusion and phreato-magmatic activity 27 March -18 May
- 3- Climactic stage with sector collapse and plinian eruption; 18 May
- 4- Declining explosive pulses; 25 May- 18 October, 1980
- 5 - Dominantly effusive stage 18 October, 1980 - October, 1986
- 6 – Intrusion stage, October 1986, September 2004

During the precursory stage, magma ascended with an average rate of 1 km/day (0.012 cm/s). The cryptodome intrusion occurred in the form of small batches of dacitic magma ascending buoyantly, residing and degassing at shallow depth for periods of weeks. The arrival of single batches is signaled by the occurrence of discrete episode of harmonic tremor. The intrusion episodes trigger also magma-water interaction with resultant phreato-magmatic activity. A break of activity occurs between April 22 and May 7, with a period characterized by the absence of episode of tremor, lack of phreatomagmatic explosion and a substantial decrease of the seismic energy release by LP earthquakes. A renewal of the above mentioned events occurs starting from May 8. This new episodes are accompanied also by a distinct increase in the deformation of the cryptodome.

A landslide on May 18, 1980 triggered a lateral blast and a plinian eruption. The first part of the eruption was fed by the cryptodome dacite, whereas the plinian phase was sustained by magma ascending directly from the magma chamber. We estimate an average ascent rate of the order of 0.6 m/s during this last phase. The plinian phase of the eruption may represent the only occurrence of a connected conduit between the deep magma chamber and the surface during the entire eruptive period. The eruption was followed by a swarm of relatively deep VT earthquakes which delineated an earthquake free volume interpreted as that of a magma chamber (Scandone and Malone, 1985). Two new eruptions on May 25 and June 12, may represent the follow up of the previous eruption with the final drainage of the conduit system. These two eruptions were preceded by only a few hours of harmonic tremor with ascent velocities comparable with that of May 18. Subsequent eruptions were caused by the ascent of single batches of magma, each characterized by its own ascent rate. Starting in June 1980, both monitoring data (seismic and gas) and sample analysis suggest that magma stored at intermediate depths; subsequent explosive eruptions included magma from deep, intermediate and shallow levels. In contrast, dome eruptions appeared to involve magma batches that resided at shallow depth for longer times. Continuous magma effusion in 1983 (a period of endogeneous dome growth) probably required full connectivity from the intermediate storage region to the surface. The precursor durations of each of these eruptions is proportional to the time of ascent of each magma batch.

The quiescence following the last dome eruption in 1986 is followed by numerous seismic swarms of VT earthquakes with depths ranging between 2 km and 9 km. We interpret these swarms as representative of repeated intrusion of batches of magma whose ascent was prevented by the presence of a barrier at 2 km depth (below datum). This barrier had been already present since the summer of 1980, but its relevance in stopping magma ascent increased with time.

Continuous accumulation of magma below this level finally achieved the breaking of the barrier with the renewal of activity in October 2005, with a precursory seismic swarm lasting for several days till the outburst of a phreatic explosion on October 1, 2004. Then first outbreak of a new dome occurred on October 11. The estimated ascent velocity from the seismic barrier are of the order of 0.001 m/s

Questions

- Is each eruption related with the ascent of single magma batches? No major eruptions require full connectivity between the magma chamber and the surface, but eruption as small as $1 \times 10^6 \text{ m}^3$ would not even fill a conduit 8 km long.
- Is the character of seismicity always the same (LP, VT)? No dome earlier eruptions were preceded mostly by LP earthquakes, whereas the last ones were preceded mostly by VT earthquakes.

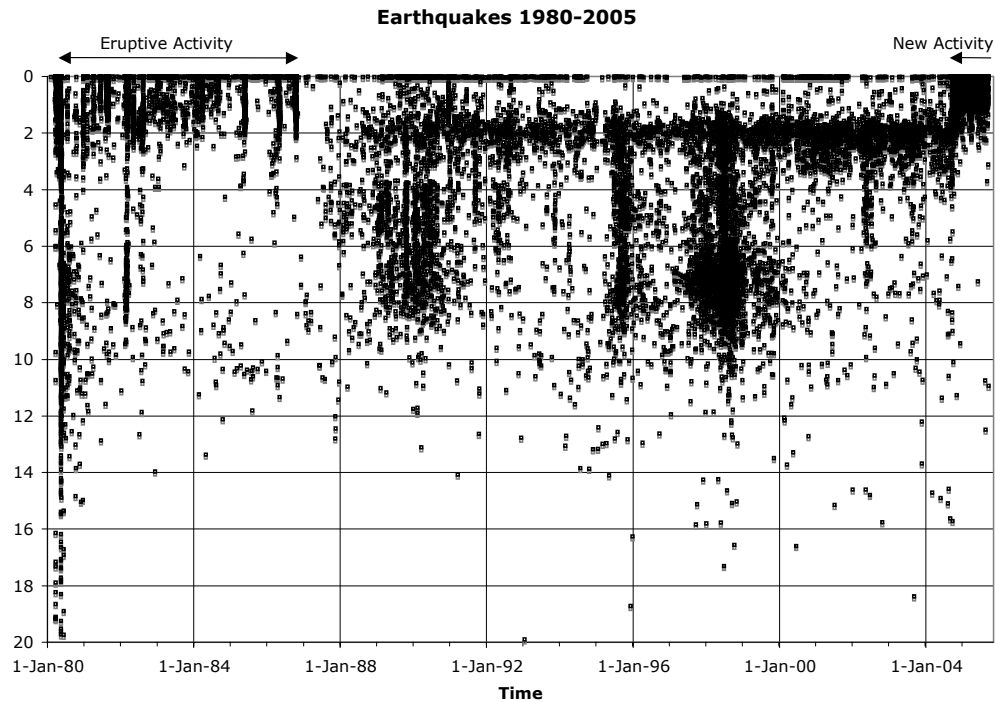


Fig. 1 – Time-Depth distribution of earthquakes at Mt St Helens in the time period 1980-2004. The seismicity after 1986 well delineates the occurrence of a barrier to the propagation of seismic swarms. (Data from Pacific North-west Seismic Network, University of Washington, Courtesy of Steve Malone)

Bibliography

- Scandone R., S.D. Malone, 1985, Magma supply, magma discharge and readjustment of the feeding system of Mount St Helens during 1980, *J. Volcanol. Geoth. Res.*, 23, 239-262
- Scandone R., Kashman C., Malone S., Fattori Speranza F., in preparation, Insights into volcano workings: Mt St Helens 1980-2004, to be submitted *Journ. Geophys. Res.*